Neutrophils induce effective antibody responses to the pneumococcal conjugate vaccine by inhibiting regulatory T cells

Essi Y. I. Tchalla, Anagha Betadpur, Andrew Y. Khalil, Elena Lopez, Manmeet Bhalla, Musea Chang, Elizabeth A. Wohlfert and Elsa N. Bou Ghanem*

Author affiliations: Department of Microbiology and Immunology, University at Buffalo School of Medicine, Buffalo, NY 14203, USA

*Address correspondence to: Elsa N. Bou Ghanem, 955 Main Street, Buffalo, NY, 14203. Telephone: 716-829-2422. Email: elsaboug@buffalo.edu

Conflict-of-interest statement: The authors have declared that no conflict of interest exists.

Abstract

We recently found that neutrophils are required for production of protective antibodies in response to the pneumococcal conjugate vaccine (PCV), however, the mechanisms behind that are not known. Here, using a mouse model, we found that depletion of neutrophils at the time of vaccination in female mice led to aberrant T cell responses in the spleen resulting in increased regulatory T cells (Tregs) that was accompanied by a dysregulated cytokine environment. We found that following vaccination, neutrophils influx into secondary lymphoid organs and increase expression of T cell engaging/inhibiting markers. When we depleted Tregs in neutrophil deficient mice at the time of vaccination, the opsonic activity of the antibodies and the ability of the sera to protect naïve hosts against pneumococcal infection significantly increased compared to controls. Importantly, we examined responses following PCV administration in human female participants and found that PCV altered neutrophil phenotype and that *in vitro* coculture of neutrophils with PBMCs at one week following vaccination resulted in lower percentage and proliferation of $FOXP3^{+}$ T cells, showing the clinical relevance of this phenotype. This work reveals a new mechanism by which neutrophils ensure protective antibody responses to vaccination by suppressing Tregs.

53 **Introduction**

54 Neutrophils or polymorphonuclear cells (PMNs) are innate immune cells that are
55 indispensable for the clearance of many infections and that have been traditionally studied as
56 anti-microbial effector cells (1). However, in the past decade, PMNs have become increasingly
57 appreciated for their ability to orchestrate adaptive immune responses (2, 3). In fact, they can
58 affect B and T cells directly or via control of antigen presenting cells such as dendritic cells and
59 macrophages (4-6). They can engage and stimulate T cells in response to antigens via expression
60 of MHC-II, CD80, CD86 and/or CD11c (7-10) or inhibit T cells via production of IL-10, reactive
61 oxygen species, arginase or by expressing PD-L1 or secreted protein acidic and rich in cysteine
62 (SPARC) (11-15). The ectonucleotidases CD73 and CD39 have been associated with T cell
63 inhibition via adenosine production and are also expressed on PMNs (16, 17). PMNs can also
64 suppress B cell responses to protein antigens (18-20) or activate B cell responses to bacterial
65 carbohydrates through secretion of B cell activating factor (BAFF), A proliferation-inducing
66 ligand (APRIL), IL-21 or Pentraxin 3 (21, 22).

67 While most of the work examining PMN interaction with adaptive immune cells have used
68 model antigens, a few studies have recently focused on the role of PMNs in vaccine responses
69 (23). In an adenovirus-SIV vaccination model of Rhesus macaques, PMNs were found to migrate
70 to the vaccine draining lymph nodes (vLNs) and acquire a B cell help phenotype as indicated by
71 expression of BAFF, IL-21 and TNFα among others (23). PMNs were found to be required for
72 effective immune responses to both tuberculosis and leishmaniasis live-attenuated vaccine
73 models (24, 25). In the context of a clinically relevant vaccine, we showed that PMNs are required
74 at the time of vaccination for induction of protective antibody responses to the licensed
75 pneumococcal conjugate vaccine (PCV) Prevnar (26). In fact, depleting PMNs at the time of PCV
76 vaccination led to a defect in antibody isotype switching to IgG2c and IgG3, a decline in antibody
77 function, and decreased ability of the mice to control and survive a subsequent pneumococcal
78 infection (26). However, the mechanisms by which PMNs control antibody responses to PCV

79 remain unclear. This is of high clinical relevance as PCV protects against infections caused by
80 the bacteria *Streptococcus pneumoniae* (pneumococcus), which remain a leading cause of
81 community acquired pneumonia globally, particularly in vulnerable populations such as older
82 adults (27). Understanding the mechanisms behind vaccine efficacy can lead to design of better
83 vaccines.

84 Conjugate vaccines such as PCV induce T follicular helper cells (Tfh) that aid the
85 production of antibodies by B cells (28, 29). In fact, PCV vaccination in humans induced the
86 formation of Tfhs, which was linked to enhanced antibody responses (30). Following vaccination
87 with a conjugate vaccine, germinal centers (GC) form and mature within secondary lymphoid
88 organs such as the lymph nodes (LNs) and spleen (31, 32). Inside GCs, polysaccharide-specific
89 B cells acquire conjugate antigens from the surface of follicular dendritic cells and process them
90 intracellularly for presentation to Tfhs (31-33). Interaction between the Tfhs and GC B cells
91 triggers B cell differentiation into antibody secreting cells and enhances antibody production, class
92 switching and affinity maturation (34, 35). These antibodies are required for efficient host
93 protection against infections as they facilitate binding, uptake and killing of bacteria by phagocytes
94 (36, 37). Antibody responses by B cells are also highly influenced by cytokines, which are
95 secreted by Tfhs as well as other T cell subsets (28, 38, 39).

96 A subset of T cells known to control immune responses are regulatory T cells (Tregs).
97 Tregs have suppressive capacity and play an essential role in homeostasis and immune tolerance
98 (40). In the context of vaccination, Tregs have been shown to limit protective immune responses
99 (41-46). In multiple HIV and cancer models of vaccination, Tregs were shown to dampen both
100 cellular and humoral immune responses, leading to viral replication or tumor progression (47, 48).
101 In a pneumococcal polysaccharides model of vaccination, blocking the Treg effector molecule
102 CTLA-4 enhanced antibody and cytokine responses to the polysaccharides (49). In humans,
103 higher Tregs in the PBMC of older adults were associated with lower $CD4^+$ T cell responses to
104 immunogenic pneumococcal proteins (50). A subset of Tregs that gain access to B cell follicles

are termed T follicular regulatory cells or Tfr (51, 52). Tfrs display phenotypic markers of T follicular helper cells (Tfhs), in addition to their expression of FOPX3 (51, 53). They play a role in humoral responses to antigens that is context dependent and have been shown to inhibit B cell responses and accelerate GC contraction (54-56). Several studies have looked at the relationship between Tregs and PMNs in models of inflammation and disease and found that Tregs modulate PMN recruitment to the site of inflammation (57-59). PMNs in turn also promote Treg recruitment in autoimmune and cancer models, and their depletion leads to a decrease in Tregs (60-63). The interaction of PMNs and Tregs during vaccine responses (including PCV) has not been studied.

In this study, we tested the effect of PMNs on adaptive immune responses to PCV using a preclinical murine model of vaccination as well as by examining responses in vaccinated human participants. We found that following vaccination, PMNs acquire a T cell engaging and suppressing phenotype and suppress Tregs, which is required for the production of protective antibodies. This study reveals a new mechanism by which PMNs shape vaccine responses through the control of Tregs and provides novel targets for the design of more effective vaccines against bacterial infections.

131 **Results**

132 **PMNs home into secondary lymphoid organs in response to PCV**

133 In prior work, we showed that PMNs are required at the time of PCV administration for the
134 induction of effective antibody response and optimal host protection against pneumococcal
135 disease (26). There is a well-documented sex-based difference in responses to PCV where
136 females elicit higher antibody responses and vaccine efficacy compared to males (64-66) and we
137 recapitulated this in preclinical murine models (67). Therefore, to understand mechanisms of
138 protection, we focused our studies on female hosts, that mount higher humoral and cellular
139 responses to PCV and are better protected against subsequent pneumococcal infection
140 compared to male hosts (67).

141 To better understand how PMNs control PCV efficacy, we first asked whether they are
142 recruited to secondary lymphoid organs (spleen and vaccine draining lymph nodes (vLNs)) in
143 response to vaccination. We looked at expression of migration markers CXCR4 and CCR7 on
144 circulating PMNs 24 hours post vaccination as they are involved in PMN trafficking to the lymph
145 nodes via the lymphatic system or high endothelial venules (Fig. S1 & Fig. 1A) (68, 69). We found
146 that at baseline, circulating PMNs express relatively low levels of both CXCR4 and CCR7 and
147 upon vaccination, expression of CCR7 increases (Fig. 1A). This higher CCR7 expression
148 coincided with a decrease in the number of circulating PMNs 18 to 24 hours post vaccination and
149 an influx of PMNs in the spleen and vLNs at those time points respectively (Fig. 1B). Following
150 the peak of PMN influx into the spleen and vLNs, PMN numbers return to baseline by 48 hours
151 post vaccination (Fig. 1B). These findings demonstrate that PMNs are rapidly recruited to
152 secondary lymphoid organs in response to PCV.

153

154 **PMNs do not affect B cell numbers in response to PCV**

155 To start investigating how PMNs induce protective antibodies to PCV, we first examined
156 changes to the B cell compartment. We depleted PMNs at the time of vaccination as presented

157 in Fig 2A and previously described (26) and investigated B cell responses in secondary lymphoid
158 organs on days 7, 14 and 21 post vaccination (Fig. S2A). Upon PMN depletion, there was no
159 change in the percentage and numbers of total B cells ($B220^+$) in the spleen compared to isotype
160 treated mice at any of the timepoints investigated (Fig. S3A). Similarly, no effect of PMN depletion
161 was observed on GC B cells ($CD38^{lo}CD96^+$) and plasmablasts ($CD138^+$) (Fig. S3B & S3C). In
162 prior work, we had observed a defect in isotype switching, opsonic and binding capacities of
163 antibodies in response to PCV in PMN deficient hosts (26), indicating a possible defect on somatic
164 hypermutation (SHM) and/or class switch recombination (CSR). Therefore, on days 7 post
165 vaccination, we assessed B cell expression of Activation Induced Cytidine Deaminase (AID), an
166 enzyme required for both SHM and CSR (70, 71) (Fig. S2B). For both total and GC B cells, there
167 was an increase in AID expression in mice following vaccination (Fig. S4). However, depleting
168 PMNs had no effect on the percentage of AID^+ B cells or the expression of AID by B cells (Fig.
169 S4). These findings suggest that PMNs are not directly acting on B cells during vaccination.
170

171 **PMNs affect MHC-II expression by macrophages and dendritic cells in response to PCV**

172 We then looked at the effect of PMNs on other immune cells important for vaccine
173 responses such as antigen presenting cells (APCs) (7, 72). For that, we depleted PMNs at the
174 time of vaccination (Fig. 2A) and analyzed the number of splenic macrophages ($F4/80^+$) and
175 dendritic cells ($DC\text{-}CD11c^+$) or their respective expression of antigen presenting molecules MHC-
176 II, CD80 and CD86 on days 7, 14 and 21 post vaccination (Fig. S5 & S6). Overall, we found that
177 depletion of PMNs had no effect on the percentages of both macrophages and DCs present in
178 the spleen (Fig. S6), except for a slight increase in macrophages in PMN-depleted mice compared
179 to PMN-sufficient mice at 21 post vaccination (Fig. S6A). A lower percentage of both
180 macrophages and DCs exprssed MHC-II in the spleen of PMN-depleted mice at day 14 post
181 vaccination compared to PMN-sufficient counterparts with no effect on CD80 and CD86
182 expression (Fig. S6). These findings suggest depletion of PMNs may impair antigen presentation.

183

184 **Absence of PMNs at the time of vaccination alters the cytokine environment in the spleen**

185 The cytokine environment in secondary lymphoid organs controls the quality of antibodies
186 produced (73). Therefore, we next looked more broadly at the overall inflammatory environment
187 in the spleen in the presence or absence of PMNs in vaccinated mice using a cytokine protein
188 array. We found that overall, in the absence of PMNs at the time of vaccination, there was an
189 increase in inflammatory mediators in the splenic milieu compared to when PMNs are present
190 (Fig. S7). This increase in inflammation was seen at day 7 and resolved by day 14 through 21
191 post vaccination (Fig. S7), timepoints that coincide with return of PMNs after depletion (26). These
192 data show that the absence of PMNs at the time of vaccination leads to an altered inflammatory
193 response in the spleen, suggesting a regulatory role for PMNs during PCV.

194 We had observed a defect in isotype switching to IgG2 and IgG3 antibodies in the absence
195 of PMNs (26), therefore, we directly tested whether PMNs controlled effective antibody response
196 to PCV through IFNγ, as this cytokine is required for class switching to those isotypes (34, 74).
197 We measured the percentage of IFNγ^+ PMNs in the spleen 18 hours post vaccination following
198 *ex vivo* stimulation with PMA, heat-killed *S. pneumoniae* or PCV (Fig. S8). We found that more
199 PMNs express IFNγ when stimulated with PMA, however, there was no change in the percentage
200 of IFNγ^+ PMNs following vaccination and upon restimulation (Fig. S9A). Similarly, total IFNγ levels
201 in the spleen within the first 28 days of vaccination were comparable between PMN-depleted and
202 PMN-sufficient mice (Fig. S9B). Additionally, when we blocked IFNγ *in vivo* at the time of
203 vaccination using an αIFNγ antibody following the same schedule as for the depletion of PMNs
204 shown in Fig. 2A, there was no effect on bacterial burden in the lung and blood at 24 hours post
205 infection (Fig. S9C) or on host survival (Fig. S9D) compared to the isotype-treated mice. To verify
206 that the blocking antibody was functioning, we measured isotype switching to IgG2 which is
207 controlled by IFNγ (34), and founded that blocking IFNγ led to an increase in IgG1 antibodies and

208 decrease in IgG2b and IgG2c (Fig. 9E). In summary, these data indicate that overall, the control
209 of pneumococcal antibody responses by PMNs is not mediated by IFNγ.
210
211 **PMNs acquire a T cell regulating phenotype upon entry into secondary lymphoid organs**
212 To better understand how PMNs control PCV efficacy, we then assessed how they
213 respond to vaccination. PMNs have been shown to acquire different phenotypes depending on
214 entry into organs/tissues and the composition of the tissue microenvironment (75, 76). Therefore,
215 we examined PMN phenotype within the first 24 hours post vaccination when they influx into
216 secondary lymphoid organs (Fig. 1B). As the cytokine responses in the spleen suggested that
217 PMNs play a regulatory role, we looked at the expression of various T cell engaging (MHC-II,
218 CD80, CD86 and Cd11c) and suppressing (PDL-1, CD73, CD39 and ARG1) markers on PMNs
219 (Fig. S1). In all sites investigated, overall, expression of both T cell engaging and suppressing
220 markers on PMNs did not change upon vaccination except for a decrease in PD-L1^{+} PMNs in the
221 blood and spleen (Fig. 3 & 4). However, there were tissue specific differences (Fig. 5). Expression
222 of CD80, CD86, CD11c MHC-II and ARG1 were higher on PMNs in secondary lymphoid organs
223 compared to circulating PMNs in both naïve and vaccinated mice (Fig. 3, 4 and 5B). These data
224 are consistent with the literature showing that entry into tissues instructs PMNs to acquire organ
225 specific phenotypes (75, 76).
226 PMNs expressing MHC-II have been reported to express a regulatory phenotype (77).
227 Therefore, we assessed the expression of CD73, CD39, ARG1, PD-L1 and SPARC on MHC-II^{+}
228 versus MHC-II^{-} PMNs (Fig. S1). In all tissues investigated, there are fewer MHC-II^{+} PMNs
229 compared to MHC-II^{-} PMNs (Fig. S10A). Those MHC-II^{+} PMNs in the spleen expressed lower
230 ARG1, higher SPARC and PD-L1 and similar levels of CD73 and CD39 compared to their MHC-
231 II^{-} PMNs in the spleen (Fig. S10B). Overall, all the above data show that upon influx into the
232 spleen and vLNs, PMNs acquire the ability to engage and suppress T cells following PCV
233 vaccination.

234

235 **PMNs do not affect T helper cell responses to PCV**

236 To test the effect of PMNs on T cell responses, we depleted PMNs at the time of
237 vaccination (Fig 2A) and measured the percentages and numbers of T helper 1 (Th1)
238 ($CD4^+TCR\beta^+FOXP3^-Tbet^+$), Th2 ($CD4^+TCR\beta^+FOXP3^-GATA3^+$), Th17 ($CD4^+TCR\beta^+FOXP3^-$
239 $ROR\gamma t^+$) and Tfh ($CD4^+TCR\beta^+CXCR5^+PD1^+$) cells and in the spleen and vLNs, 7-, 14- and 21-
240 days post vaccination (Fig. S11). Except for an increase in the percentage of Th1 cells in the
241 spleen of PMN-depleted mice (Fig. S12A), we found that there was no difference in the
242 percentages or numbers of Th2, Th17 and Tfhs between vaccinated PMN-depleted and PMN-
243 sufficient mice at any the timepoints investigated in the spleen (Fig. S12B-D). As examining total
244 $CD4^+$ T cells may mask changes within the smaller antigen experienced population, we also
245 looked at antigen experienced cells by gating on $CD49d^+CD11a^+$ T cells (Fig. S11A) (78).
246 Similarly, we found no effect of PMN depletion on antigen experienced Th1, Th2, Th17 and Tfhs
247 in the spleen (Fig. S13).

248 As depleting PMNs had no effect on the amount of T helper cells (Fig. S12 & S13), we
249 asked if their ability to produce cytokines was impaired. We examined cytokine responses *ex vivo*
250 using PMA/Ionomycin as positive stimulant for cytokine production. Using flow cytometry, we
251 measured expression of IFNγ, IL-4, IL-17, TGFβ and IL-10 by splenic $CD44^{hi}$ activated $CD4^+$ T
252 cells at day 14 post vaccination (Fig. S14). We used the protein Latency Associated Peptide (LAP)
253 as a proxy for TGFβ production since it acts as a chaperone for TGFβ and their levels correlate
254 (79, 80). The cytokine response was skewed towards production of IFNγ and LAP, both in the
255 presence and absence of PMNs, as the percentage of CD4+TCRβ+ T cells expressing these
256 cytokines was higher than the other cytokines investigated (Fig. S15). Overall, PMA/Ionomycin
257 stimulation increased LAP, IFNγ and IL-4 expression by $CD44^{hi}$ $CD4^+$ T cells above the no

258 stimulation condition (Fig. S15A-C). However, PMN depletion did not affect expression of any of
259 the cytokines by T cells in comparison to PMN-sufficient mice (Fig. S15).
260
261 **PMNs inhibit Treg expansion in the spleen in response to PCV**
262 We next assessed the effect of PMNs on regulatory T cells (Tregs) ($CD4^+TCR\beta^+FOXP3^+$)
263 and T follicular regulatory cells (Tfrs) ($CD4^+TCR\beta^+CXCR5^+PD1^+FOXP3^+$) following PCV (Fig. 6).
264 We saw an increase in the percentage of Tregs in the spleens of PMN-depleted mice compared
265 to PMN-sufficient mice at day 14 post vaccination (Fig. 6A). In PMN-depleted mice, there was
266 also an increase in the percentage and numbers of Tfrs at days 21 & 7 post vaccination
267 respectively (Fig. 6B). When looking at the antigen experienced compartment, there was an
268 increase in Tregs and Tfrs at day 14 post vaccination in the spleen of PMN-depleted mice
269 compared to PMN-sufficient mice (Fig. 6C & 6D). These data suggest that PMNs inhibit the
270 expansion of regulatory T cells in the spleen following PCV.
271
272 **PMNs inhibit Treg expansion in response to PCV *in vitro***
273 To directly assess the effect of PMNs on Tregs, we used *in vitro* assays. For that, we
274 performed coculture assays of splenocytes isolated from day 1-vaccinated mice in the presence
275 or absence of PMNs using heat-killed bacteria or αCD3 as stimulants for 48 hours. PMNs were
276 removed from splenocytes using positive isolation magnetic sorting. Similar to what we observed
277 *in vivo*, in the absence of PMNs, there was an increase in the percentage of Tregs in response to
278 stimulation with heat-killed *S. pneumoniae* (Fig. 7). PMN removal did not alter other T helper cell
279 subsets (Fig. S16). This recapitulates the *in vivo* findings and suggests that PMNs control Tregs
280 response to bacterial polysaccharides.
281
282 **Reducing Tregs in PMN-depleted hosts rescues antibody responses**

283 Next, we tested whether the increase in regulatory T cells is responsible for the defective
284 antibody responses seen in the absence of PMNs at the time of vaccination (26). To investigate
285 this, we depleted Tregs using an αCD25 antibody (81) either alone or in conjunction with PMN
286 depletion using αLy6G (Fig. 2B). We achieved ~90% depletion of PMNs in the blood and ~40-
287 50% depletion of Tregs in both spleen and blood (Fig. S17A & S17B). Moreover, αCD25 and
288 αLy6G injections had no effect on percentages of Th1, Th2, Th17, Tfhs and B cells in the spleen
289 (Fig. S17C).

290 We then followed antibody levels upon Treg and/or PMN depletion in the blood of mice at
291 weeks 0, 2 & 4 post vaccination. We found an increase in total IgG against pneumococcal
292 polysaccharides in PMN-& Treg-depleted mice compared to PMN-depleted mice at 4 weeks post
293 vaccination (Fig. 8A). We next investigated the ability of antibodies in the sera to bind the surface
294 of the pneumococcus (Fig. S18). In all mouse groups, vaccination significantly increased binding
295 of IgG to the bacteria compared to baseline (Fig. 8B). As previously reported, sera from
296 vaccinated PMN-depleted mice had significantly lower IgG binding compared to sera from
297 vaccinated PMN-sufficient mice (Fig. 8B) (26). Interestingly, depletion of Tregs in PMN-depleted
298 mice rescued IgG binding in the sera to similar levels to that of PMN-sufficient vaccinated mice,
299 while depletion of Tregs alone had no effect (Fig. 8B). We also looked at the ability of antibodies
300 in the sera to promote opsonophagocytic killing of the pneumococcus by PMNs isolated from
301 naïve mice. As expected, there was an increase in bacterial killing by PMNs when sera from
302 vaccinated versus naïve mice were used as opsonins (Fig. 8C). We also found that sera from
303 PMN-depleted mice induced lower bacterial opsonophagocytic killing by PMNs compared to sera
304 from PMN-sufficient mice (Fig. 8C). Similar to above, depletion of Tregs in PMN-depleted mice
305 rescued the ability of the sera to induce opsonophagocytic bacterial killing to levels similar to
306 PMN-sufficient vaccinated mice, while depletion of Tregs alone did not affect opsonic capacity
307 (Fig. 8C).

308 To confirm these findings, we used a different model of Treg depletion for assessment of
309 antibody responses to PCV using diphtheria toxin (DT) mediated depletion (82). For that, we used
310 DT injections to deplete Tregs either alone or in conjunction with PMN depletion in DEREG mice
311 (83) (Fig. S19A). We achieved ~25% depletion of Tregs in the spleen (Fig. S19B). Treg depletion
312 in PMN-depleted DEREG mice increased their IgG levels 4 weeks post vaccination compared to
313 vehicle treated PMN-depleted mice (Fig. S19C). The above data suggest that the increase in
314 Tregs seen in PMN-depleted mice contributes to the defective antibody response observed in
315 these mice as reduction of the Tregs rescues the levels and function of the antibodies to similar
316 levels seen in PMN-sufficient vaccinated mice.
317
318 **Reducing Tregs in PMN-depleted hosts rescues the protective capacity of the sera against**
319 **pneumococcal infection**
320 Finally, we assessed the protectiveness of the sera from PMN- and/or Treg-depleted mice
321 *in vivo* against infection by adoptively transferring sera from each group into naïve mice. Recipient
322 mice were then infected 1hr later with $3x10^5$ CFU of *S. pneumoniae* TIGR4 strain, assessed for
323 blood bacterial burden 48 hours post infection and monitored for survival. Recipients of sera from
324 vaccinated PMN-sufficient mice were able to control bacterial numbers better than the ones
325 receiving sera from vaccinated PMN-depleted mice with 50% and 87.5% of the mice becoming
326 bacteremic respectively (Fig. 9A). Receiving sera from PMN- & Treg-depleted mice rescued the
327 ability of the recipients to control infection with only 25% of the mice becoming bacteremic (Fig.
328 9A). Additionally, receiving sera from Treg-depleted mice did not affect control of blood bacterial
329 burden (Fig. 9A). Looking at survival, only 10% of recipients of sera from naïve mice survived the
330 infection compared to ~70% of the recipients of sera from vaccinated PMN-sufficient mice (Fig.
331 9B). Receiving sera from PMN-depleted mice resulted in only 30% survival, compared to ~81%
332 survival of mice that received sera from PMN- & Treg-depleted mice (Fig. 9B). The above data

333 suggest that reduction of Tregs in PMN-depleted mice rescues the protectiveness of the sera to
334 levels similar to PMN-sufficient vaccinated mice.
335
336 **Vaccination of human participants alters the phenotype of circulating PMNs**
337 As PMN responses vary significantly across species (84), we wanted to test the clinical
338 relevance of these findings. To do so we recruited unvaccinated adult female participants,
339 administered PCV to them, and monitored the phenotype of PMNs in the circulation over time in
340 response to vaccination by examining the expression of T cell engaging and inhibiting markers
341 using flow cytometry (Fig. S20). To test if PMNs respond to PCV and alter their phenotype, we
342 used the OMIQ software to perform opt-SNE analysis to visualize the data, and cluster them using
343 FLOWSOM. We found that PMNs separated into different clusters with varying levels of maturity
344 (based on CD10 expression, Fig. 10A and S21) with cluster 6 being highest followed by 3, 2, 4,
345 1, 9, 7, 5, and 8 the lowest. Clusters 6 (most mature) was the only cluster that expressed PDL-1
346 and had high levels of all the other markers, while cluster 8 (least mature), did not express any of
347 the markers we tested (Fig. 10A, 10C and S21). Upon vaccination, we observed a shift in the
348 abundance of circulating clusters where cluster 1, 2 and 6 decreased in abundance, cluster 3, 4
349 and 5 increased, while cluster 7 and 8 did not change (Fig. 10B). The clusters that decreased
350 from the circulation expressed the highest levels of CD39, ARG1 and HLADR (Fig. 10C) and may
351 be homing to the tissues as we observed in mice. When we examined the expression levels of
352 the various markers at week 1 following vaccination, we found that expression of HLADR, CD86,
353 CD39 and PDL-1 increased on all the clusters that expressed them, CD73 either increased or
354 decreased depending on the cluster, while ARG1 decreased (Fig. 10C). Overall, these findings
355 suggest that in response to PCV in humans, the phenotype of circulating PMNs changes, where
356 particular clusters increase expression of T cell engaging and suppressing markers and possibly
357 exit from the circulation into tissues.
358

359 **PMNs from PCV immunized donors inhibit FOXP3$^+$ T cell expansion *in vitro***

360 Finally, we tested whether PMNs from vaccinated participants can suppress FOXP3$^+$
361 CD4$^+$ T cells. For that, at one week post vaccination, a timepoint where we observed phenotypic
362 changes in PMNs in response to vaccination (Fig. 10), we performed an *in vitro* assay where
363 PBMCs from each participant were cocultured with or without PMNs (from the same donor) and
364 stimulated with PCV for 48 hours (Fig. S22). Similar to what we found in the preclinical model,
365 the presence of PMNs resulted in reduction of FOXP3$^+$ T cells. Addition of PMNs to PBMC
366 cultures lead to a decrease in the percentages of total and antigen experienced FOXP3$^+$ T cells
367 in 67% of participants (Fig. 11A). We also observed a decrease in Ki67$^+$ antigen experienced
368 FOXP3$^+$ T cells in the presence of PMNs in 100% of the participants (Fig. 11B), suggesting that
369 PMNs were suppressing proliferation. These data suggest that PMNs inhibit FOXP3$^+$ T cell
370 responses in humans following PCV administration.
371
372
373
374
375
376
377
378
379
380
381
382
383
384

385 **Discussion**

386 There are a growing number of studies investigating the effect of neutrophils on adaptive
387 immune responses with a few of them focusing on vaccine responses (23-25). In this study, we
388 report a new mechanism by which PMNs control antibody responses to the clinically relevant PCV
389 by controlling Treg numbers. In fact, when neutrophils were depleted at the time of PCV
390 vaccination, there was an expansion in the number of Tregs that resulted in a defect in protective
391 antibody responses (26). Reduction of Tregs in PMN-deficient vaccinated mice boosted antibody
392 number, function, and protective efficacy in the sera. This work demonstrates that PMNs drive
393 production of functional antibodies against pneumococci in response to PCV by limiting the
394 expansion of immune suppressive Tregs.

395 While the effect of PMNs on Tregs has not been investigated in the context of clinically
396 relevant vaccines, several studies have looked at the relationship between Tregs and PMNs in
397 models of inflammation and disease (57-63). Here we report that PMNs can inhibit Tregs, which
398 is in contrast to prior work demonstrating that PMNs promote Tregs in models where high level of
399 inflammation is induced (60, 61, 63). The exact way by which PMNs inhibit Tregs in response to
400 PCV remains to be elucidated, however multiple mechanisms could be involved. Some
401 possibilities could be via control of the transcription factor FOXP3, a master regulator of Treg
402 induction and function (85, 86) or control of cytokines required for Treg differentiation and viability.
403 In traumatic brain injury patients, release of serine proteases (neutrophil elastase and proteinase
404 3) by infiltrating PMNs cleaved cytokine receptors on the surface of T cells including IL-2Rα, the
405 IL-2 receptor subunit that is important for IL-2 signaling in Tregs (87, 88). In addition, those
406 proteases can cleave cytokines themselves including TGFβ and IL-2, leading to limited activation
407 of T cell response (89, 90). In response to PCV, PMNs may similarly inhibit Treg induction by
408 release of their proteases to deplete Treg-inducing cytokines and/or their respective receptors on
409 the surface of Tregs. Weak antigenic TCR stimulation on naïve T cells in the presence of TGFβ
410 can lead to Treg production via induction of FOXP3 (91, 92). We found that in the absence of

411 PMNs, a lower percentage of macrophages and DCs express MHC-II, which can weaken the
412 TCR-MHC-II interaction by lowering antigen density on the surface of the antigen presenting cell
413 (93). Therefore, the presence of PMNs at the time of vaccination can lead to Treg suppression by
414 increasing the strength of APC interaction with T cells through high MHC-II expression. Signaling
415 of retinoic acid (RA) in naïve T cells enhances TGFβ-mediated induction of Tregs (94) and RA
416 boosts PMN anti-bacterial functions (95). It is possible that RA sequestration by PMNs limits its
417 availability for Treg induction. PMNs could also be inhibiting Tregs through release of their granule
418 component cathelicidin antimicrobial peptide, the human form of which (LL-37) was shown to
419 induce Treg apoptosis *in vitro* (96). Alternatively, PMNs could be suppressing Tregs through the
420 release of miRNA containing extracellular vesicles (EVs). PMN-derived EVs containing miRNAs
421 have been shown to modulate responses in other cells including macrophages and endothelial
422 cells (97-99). The absence of miRNA-146a has been shown to promote Treg expansion, and
423 other miRNAs are known to control Treg induction (100, 101). PMNs, which express miRNA-146a
424 among others (102, 103), could use such mechanism to limit Treg expansion. All these potential
425 mechanisms can be avenues of future research for this work.

426 The findings here suggest that the expanded Tregs in PMN-depleted mice are detrimental
427 and contribute to the defective antibody responses. In general, Tregs have been shown to
428 negatively affect immune responses to vaccines. Depletion of Tregs using αCD25 in vaccination
429 models against herpes simplex virus (HSV) and *Plasmodium berghei*, increased $CD8^+$ T cell
430 responses to their respective vaccine epitopes and led to increase protection against subsequent
431 challenge with the respective pathogens (43, 104). In humans, responses to an experimental
432 vaccine of dendritic cells loaded with HIV peptides (105) found that patients with lower levels of
433 HIV-specific Tregs displayed better T-effector cell responses following vaccination (48). In the
434 context of *S. pneumoniae*, blocking of CTLA-4, an effector molecule on Tregs, enhanced levels
435 of antibodies against pneumococcal polysaccharides in immunized mice and higher Tregs in older
436 adults were associated with decreased proliferation of $CD4^+$ effector T cells in response to the

437 pneumococcal protein AliB (49, 50). Additionally, Tfrs, which we found are increased in PCV-
438 vaccinated PMN-depleted mice, have been shown to inhibit B cells responses and promote the
439 contraction of GC reactions (54, 56). The findings here, showing an improvement of vaccine
440 response upon depletion of the expanded Tregs in PMN-depleted mice, are in line with the
441 reported inhibitory role of Tregs in vaccine responses.

442 There have been several studies examining how Tregs and Tfrs inhibit B cell responses
443 (106). They can affect B cell number, differentiation, and antibody responses via release of
444 soluble mediators such as the neuropeptide neuritin, IL-10 and TGFβ or through contact
445 dependent mechanisms involving CTLA4, PD1 and granzymes (106-108). This suppression can
446 lead to a decrease in B cell expression of activation-induced deaminase (AID) (109). However, B
447 cell numbers and AID expression were not affected in this study. It is possible that the DNA
448 binding capacity or the enzymatic activity of AID are affected instead. AID activity is regulated by
449 its phosphorylation status which can either enhance or inhibit its enzymatic activity, depending on
450 the amino acid being phosphorylated (110, 111) by protein Kinase A (PKA) (112-115). It is
451 therefore possible for Tregs to be regulating AID phosphorylation in response to PCV, rather than
452 overall expression through modulation of cAMP as they have been shown to do in DCs and
453 effector T cells (116).

454 We found that the phenotypes observed in the preclinical model are also found in human
455 participants, highlighting the clinical relevance of this work. Upon vaccination of healthy human
456 donors, PMNs in the circulation changed phenotype suggesting they are responsive to
457 vaccination. Using peripheral blood collected from donors after PCV vaccination for *in vitro*
458 cocultures, addition of PMNs to PBMCs lead to a reduction in $FOXP3^{+}$ T cells and their
459 proliferation, recapitulating the Treg inhibiting property of PMNs seen in the mouse models.
460 However, further clinical studies are needed to assess the *in vivo* role of PMNs in protecting
461 human hosts against pneumococcal disease, including linking PMN phenotype to antibody
462 responses. Nevertheless, these findings can impact the design of improved pneumococcal

463 vaccine formulations that offer better efficacy, especially in the more vulnerable populations.
464 Despite their availability, pneumococcal vaccines do not mitigate the growing global burden of *S.*
465 *pneumonia* infections (27, 65, 117). This is due in part to the fact that the vaccines do not protect
466 all populations equally, where male donors and aged individuals mount lower responses
467 compared to female counterparts. Interestingly, Tregs are reported to be higher in males
468 compared to sex-matched females and higher in older adults compared to younger people (118-
469 120). In this work, we identified the role of the PMN-Treg axis in controlling antibody responses
470 in females that can be targeted for improvement of current vaccine formulations moving forward.
471 While further studies are needed to tease apart the specific mechanisms behind this inhibition of
472 Tregs by PMNs, the findings have important implications for development of future vaccine
473 strategies to improve efficacy to infections. Indeed, this PMN-Treg axis can be further studied in
474 the context of sex and age-driven differences in vaccine responses (121, 122) and can be targeted
475 to increase vaccination efficacy in the vulnerable older adults and male populations. The exact
476 mechanisms of Treg inhibition by PMNs need to be elucidated to pinpoint what pathways or
477 molecules to target specifically in the future.
478
479
480
481
482
483
484
485
486
487
488

489 **Methods**

490 **Mice**

491 Adult (10-12 weeks old) female C57BL/6 mice were purchased from Jackson Laboratories (Bar
492 Harbor, Maine). Our study focused on female hosts, as there is a well-documented sex-based
493 difference in responses to PCV where females elicit higher antibody responses and are better
494 protected from subsequent infection compared to males (64, 67, 123). Therefore, we examined
495 the mechanisms behind vaccine efficacy in the better protected hosts. Ongoing work in our lab is
496 focused on sex-based difference in PMN responses in vaccinated hosts (67) which is beyond the
497 scope of this study. Adult (10-16 weeks old) C57BL/6-Tg(Foxp3-DTR/EGFP)23.2Spar/Mmjax
498 DEREG mice were a kind gift from Elizabeth Wohlfert and have been previously described in
499 detail (82, 83). All mice were housed in a specific-pathogen-free environment at the University at
500 Buffalo Jacobs School of Medicine and Biomedical Sciences animal facility.

501

502 **Immunization and sera collection**

503 Mice were vaccinated intramuscularly with 50ul of the Polysaccharide Conjugate Vaccine Prevnar
504 13 (Wyeth Pharmaceuticals) into the caudal thigh muscle. 10ul of blood from each mouse was
505 collected from the tail at weeks 0, 2 and 4 following vaccination and used for assessment of
506 antibody titers. Sera from each mouse group were collected via cardiac puncture 4 weeks
507 following vaccination, pooled and aliquoted to assess antibody quantity and functions in
508 subsequent assays.

509

510 **Bacteria**

511 *Streptococcus pneumoniae* TIGR4 strain (serotype 4) was a kind gift from Andrew Camilli.
512 Bacteria were grown to mid-exponential phase in Todd–Hewitt broth (BD Biosciences)
513 supplemented with Oxyrase at 37°C/5% carbon dioxide, aliquoted in growth media supplemented
514 with 20% glycerol and saved at -80°C as previously described (26, 67). Prior to use, bacteria were

515 thawed on ice, washed, and enumerated by serial dilution in PBS followed by dribbled plating on
516 Tryptic Soy Agar (TSA) plates supplemented with 5% sheep blood (Northeast Laboratory
517 Services).
518
519 **Neutrophil depletion**
520 Mice were injected intraperitoneally with 50μg of the Ly6G-depleting antibody IA8 or isotype IgG
521 control following the same schedule as shown in Fig. 2A and previously described (26).
522
523 **Regulatory T cell depletion**
524 B6 mice were treated intraperitoneally with 300μg of the CD25-depleting antibody PC-61.5.3 or
525 isotype IgG1 control following the schedule shown in Fig. 2B. DEREG mice were treated
526 intraperitoneally with 1μg of diphtheria toxin (Millipore) or DMSO as vehicle control following the
527 schedule shown in Fig. S18A. Depletion efficiency was assessed by flow cytometry (Fig. S16 &
528 S18A).
529
530 **Murine organ/tissue processing and flow cytometry**
531 Blood, spleens and/or vaccine draining lymph nodes (vLNs- inguinal and popliteal) were
532 harvested from euthanized mice. Single cell suspensions from spleens and vLNs were prepared
533 in RPMI 1640 media supplemented with 10% Fetal Bovine Serum. Following red blood cells lysis
534 with an in-house hypotonic solution (8.29g ammonium chloride, 1g sodium bicarbonate, 0.038g
535 trypsin/ethylenediaminetetraacetic acid (EDTA) and 1L of water), the remaining cells were
536 enumerated, incubated with Fc block (2.4G2), Live/Dead dye (Invitrogen) and stained with
537 additional antibodies in separate panels.
538 For PMNs, cells were stained with Ly6G (1A8), CD11b (M1/70), CXCR4 (2B11), CCR7
539 (4B12), CD80 (16-10A1), CD86 (GL1), CD11c (N418), MHC-II (M5/114.15.2), SPARC (124413),

540 PD-L1 (MIH5), CD39 (24DMS1) and/or CD73 (TY/11.8) antibodies followed by permeabilization
541 with Cytofix/Cytoperm (BD) and intracellular staining with ARG1 (A1exF5).
542 For B cells, cells were stained with CD45R/B220 (RA3-6B2), CD138 (281-2), CD95
543 (SA367H8), and CD38 (90) antibodies followed by permeabilization with Fix/Perm buffer from the
544 FOXP3/Transcription factor staining buffer set (eBioscience) and intracellular staining with AID
545 (Polyclonal, Bioss).
546 For T cells, cells were stained with CD4 (RM4-5), TCRβ (H57-597), CD11a (M17/4),
547 CD49d (R1-2), PD1 (J43) and/or CXCR5 (SPRCL5) antibodies followed by permeabilization with
548 Fix/Perm buffer from the FOXP3/Transcription factor staining buffer set (eBioscience) and
549 intracellular staining with FOXP3 (FJK-16s), RORγT (931-378), Tbet (eBio4B10) and GATA3
550 (L580-823).
551 For intracellular cytokine staining in PMNs, cells were incubated in Brefeldin A in RPMI
552 1640 media supplemented with 10% Fetal Bovine Serum and 1% Pen/Strep and stimulated with
553 $9x10^6$ CFU/well of heat-killed *S. pneumoniae* TIGR4 strain, 10µl/well of PCV, 100nM of phorbol-
554 12-myristate 13-acetate (PMA) or media alone for 3 hours. Cells were then washed and stained
555 extracellularly with Fc block, Live/Dead dye, Ly6G, and CD11b antibodies followed by intracellular
556 staining with IFNγ (XMG1.2) after permeabilization with Cytofix/Cytoperm (BD). For intracellular
557 cytokine staining in T cells, cells were incubated in Brefeldin A (BD) in RPMI 1640 media
558 supplemented with 10% Fetal Bovine Serum and 1% Pen/Strep and stimulated with a mix of 81nM
559 of PMA and 1.34µM of Ionomycin (Cell activation cocktail, Biolegend) or media alone for 2 hours.
560 Cells were then washed and stained extracellularly with Fc block, Live/Dead dye, CD4, TCRβ,
561 CD44 (IM7) and LAP (TW7-16B4) antibodies followed by intracellular staining with IFNγ
562 (XMG1.2), IL-17 (931-378), IL-4 (11B11) and IL-10 (JES5-16E3) antibodies after permeabilization
563 with Fix/Perm buffer from the FOXP3/Transcription factor staining buffer set (eBioscience).
564 Following staining, cells were washed with FACS buffer (HBSS, 1% FBS and 0.1% sodium azide)

565 and fluorescence was assessed using a BD Fortessa. At least 20,000 cells in the live, $CD4^+TCR\beta^+$
566 and $B220^+$ cells gates respectively were collected and analyzed using the FlowJo software.
567
568 **Antibody Enzyme-Linked Immunosorbent Assay**
569 Antibodies in sera were assessed using an ELISA assay as previously described (26, 124).
570 Briefly, Nunc-maxisorp plates (Thermo Scientific) were coated at 4°C overnight with type 4
571 Pneumococcal Polysaccharide (ATCC®) at 2µg/well. The next day, plates were washed in PBS
572 supplemented with 0.25% Tween (PBS/T) and sera preabsorbed with a pneumococcal cell wall
573 polysaccharide mixture (CWP-multi, Cederlane) were added to the plates. After a 2-hour
574 incubation, plates were washed and incubated with diluted horseradish peroxidase (HRP)
575 conjugated anti-mouse IgM (Invitrogen), IgG (Millipore Sigma) or IgG1, IgG2b, IgG2c or IgG3
576 (Southern Biotech). One hour later, plates were washed, TMB substrate (Thermo Scientific) was
577 added, and absorbance was read at 650nm using a Biotek microplate reader for 10 minutes at 1-
578 minute intervals. Antibody units were calculated as a percentage of standard sera included in
579 each assay. Standard sera were obtained from mice that were intranasally inoculated with *S.*
580 *pneumoniae* serotype 4 weekly for 3 weeks and immunized with PCV at week 4.
581
582 **IFNγ Enzyme-Linked Immunosorbent Assay**
583 Single cell suspension of splenocytes were prepared in 2ml of RPMI 1640 media supplemented
584 with 10% Fetal Bovine Serum. IFNγ concentrations were quantified using the Mouse IFNγ ELISA
585 kit (Invitrogen, KMC4021) per manufacturer's instructions.
586
587 **IFNγ blocking *in vivo***
588 Mice were treated intraperitoneally with 200µg of the IFNγ-blocking antibody XMG1.2 or isotype
589 control following same schedule as neutrophil depletion shown in Fig. 2A.

590

591 **Cytokine/Chemokine Array**

592 Pan cytokines were assessed using the Proteome Profiler Mouse XL Cytokine Array kit (R&D,
593 ARY028) following the manufacturer's instructions as previously described (26). Briefly, single
594 cell suspension of splenocytes were prepared in 2ml of RPMI 1640 media supplemented with
595 10% Fetal Bovine Serum. Cell suspensions were aliquoted and saved at -80°C. Samples were
596 thawed on ice prior to use, lysed with Triton-X (VWR, 0694) and quantified for protein
597 concentrations using the Pierce BCA protein assay kit (Thermofisher, A55864) per the
598 manufacturer's instructions. All samples were brought to the same protein concentrations and
599 used for pan-cytokine assessment. Protein membranes were read using the BioRad ChemiDoc
600 MP Imaging System and the intensity for each dot on the blots was quantified using the Quick
601 Spots Image Analysis Software. The intensity values of each blot were blanked using their
602 respective buffer only controls. Intensity values across multiple blots were normalized using the
603 blot with the highest standard. Fold change of the values from vaccinated PMN-depleted mice
604 over those of vaccinated PMN-sufficient mice were calculated and log transformed.

605

606 **Splenocyte culture assays**

607 For mice, single cell suspension of splenocytes were prepared in 2ml of RPMI 1640 media
608 supplemented with 10% Fetal Bovine Serum one day post vaccination. To remove PMNs from
609 the obtained suspensions, splenocytes were stained with a PE labeled anti-Ly6G antibody and
610 treated using the EasySep™ Release Mouse PE Positive Selection Kit (StemCell) following
611 manufacturer's instruction. One million cells per conditions were used and treated with $5x10^7$ CFU
612 heat-killed *S. pneumoniae* or 1µl/ml αCD3 (positive control). Cells were cocultured for two days
613 before assessing percentages of Tregs.

614

615 **Antibody binding to the surface of *S. pneumoniae***

616 Sera collected 4-weeks post vaccination were used to assess antibody binding to *S. pneumoniae*
617 (TIGR4) as previously described (26, 67). After 30 minutes of incubation at 37°C, cells were
618 washed with FACS buffer and labeled with an APC-tagged anti-mouse IgG (polyclonal) antibody
619 for 30 minutes on ice in the dark. Cells were then washed, resuspended in FACS buffer and
620 fluorescence was assessed using a BD Fortessa. At least 10,000 cells were analyzed using the
621 FlowJo software.
622
623 **Opsonophagocytic Killing Assay (OPH)**
624 Neutrophils were isolated from the bone marrow of mice using density centrifugation with
625 Histopaque 1119 and Histopaque 1077 (Sigma) as previously described (26, 124, 125). Briefly,
626 Neutrophils were resuspended in HBSS (without Ca^{2+} or Mg^{2+}) media supplemented with 0.1%
627 gelatin and used in the assay. Sera collected 4-weeks post vaccination were incubated with *S.*
628 *pneumoniae* TIGR4 for 5 minutes and added to neutrophils in HBSS (with Ca^{2+} and Mg^{2+}).
629 Following a 40-minute incubation at 37°C, reactions were plated on TSA plates with 5% sheep
630 blood. Percent killing was calculated relative to a no neutrophils control for each sera condition.
631
632 **Adoptive Transfer of Sera**
633 Four weeks following immunization, naïve, vaccinated neutrophil- and Treg-sufficient, neutrophil-
634 depleted, neutrophils- and Treg-depleted and Treg-depleted were euthanized. Blood was
635 harvested via cardiac puncture; sera were obtained from the blood and pooled for each mouse
636 group. A volume of 250µL of sera was transferred intraperitoneally into naive recipients which
637 were infected 1hour later.
638
639 **Animal Infections**
640 Mice were infected intratracheally with $3x10^5$ CFU of *S. pneumoniae* serotype 4 (TIGR4) using
641 the tongue pull method as previously described (26, 126). Mice were monitored for survival for a

642 total of 7 days post infection and assessed daily for bacteremia by plating blood collected in 50mM
643 EDTA on blood agar plates for enumeration of bacterial CFU.
644
645 **Human participants**
646 Healthy unvaccinated female participants (24-29 years old) were recruited under NCT06128915.
647 Individuals who were pregnant, had acute infections within the last 2 weeks, took medication 48
648 hours prior, had history of chronic infections, had conditions that altered immunity (autoimmunity,
649 on immune modulating drugs, history of cancer) were excluded from the study. At the first visit
650 (week 0), donors had their blood drawn then were administered the Polysaccharide Conjugate
651 Vaccine Prevnar 20 (Pfizer, Wyeth Pharmaceuticals) intramuscularly as per manufacturer's
652 instructions. At week 1 and 4 following vaccination, donors had their blood drawn for subsequent
653 PMN phenotyping. Blood from week 1 was also used for coculture assays. All blood was collected
654 into tubes containing sodium citrate and visits occurred in the morning (8AM-10AM) to control for
655 circadian variations in PMN phenotype (127). All enrolled participants signed approved informed
656 consent forms.
657
658 **Human PMN isolation and flow cytometry**
659 For participants, PMNs were isolated from peripheral blood of week 0, 1, 4 post vaccinated
660 donors using EasySep™ Direct Human Neutrophil Isolation Kit (StemCell) respectively following
661 manufacturers' instructions. For each donor and visit $1x10^5$ PMNs were added to each well and
662 then stained with CD16 (eBioCB16), CD14 (61D3), CD10 (MEM-78), HLA-DR (L243), CD86
663 (BU63), PDL1 (MIH1), CD73 (AD2), CD39 (124413), PD-L1 (MIH5), CD39 (eBioA1) and/or CD73
664 (TY/11.8) antibodies followed by permeabilization with Cytofix/Cytoperm (BD) and intracellular
665 staining with ARG1 (A1exF5). Following staining, cells were washed with FACS buffer and
666 fluorescence was assessed using a BD Fortessa. At least 5000 cells in the $CD16^+$ gate were
667 collected and analyzed using the FlowJo software.

668

669 **Human PMN FLOWSOM analysis**

670 Analysis and data visualization of the PMN phenotype with and without vaccination over time was
671 completed using a software OMIQ (Dotmatics). Traditional gating was done to differentiate the
672 neutrophil population and all the markers. Dimensional reduction was next performed with
673 optimized parameters for T-distributed stochastic neighbor embedding which improves
674 visualization of large datasets by reducing it to 2D/3D map while preserving local structure.
675 Clustering into neutrophil subsets was done using Flow-cytometry specific self-organizing map
676 (FLOWSOM) algorithm. Clustered heat maps were made based on meta-cluster gating to
677 characterize the different PMN subsets based on the expression of different markers.

678

679 **Human PMN/PBMC coculture assays**

680 For participants, PBMCs and PMNs were isolated from peripheral blood of 1-week
681 vaccinated donors using the One-Step Polymorph (Accurate Chemical) and EasySep™ Direct
682 Human Neutrophil Isolation Kit (StemCell) respectively following manufacturers' instructions. For
683 each donor, $2x10^5$ PBMCs were incubated in (RPMI with 10% FBS) with or without addition of
684 $5x10^4$ PMNs and stimulated with 10µl of PCV. Cells were cocultured for two days before
685 assessing percentages and proliferation of T cells**.** At 48 hours post incubation, T cells were
686 stained with CD11a (HI111), PD1(EH12.1), CD4(S3.5), CD49d (9F10), CXCR5 (MU5UBEE),
687 CD25 (BC96) followed by permeabilization with Fix/Perm buffer from the FOXP3/Transcription
688 factor staining buffer set (eBioscience) and intracellular staining with FOXP3 (PCH101), RORγT
689 (AFJKS-9), Tbet (eB4B10), GATA3 (L580-823) and ki67 (B56). Following staining, cells were
690 washed with FACS buffer and data collected using a BD Fortessa. At least 10,000 cells in the live
691 $CD4^+$ gate were collected and analyzed using the FlowJo software.

692

693 **Statistical Analysis**

All statistical analysis was done using GraphPad Prism version 10 software. Data were checked for normality distribution using the Shapiro-Wilk test. Significant differences were determined by One-way analysis of variance followed Šídák's, Holm-Šídák's, Tukey's or Dunnett's multiple comparisons test; Kruskal-Wallis One-way analysis of variance followed Dunn's multiple comparisons; Mann-Whitney test or Student's t test; or one sample t-test as appropriate. Survival was analyzed using the log-rank (Mantel-Cox) test. All p values <0.05 were considered significant.

Study Approvals

All work with mice was performed in accordance with the recommendations in the Guide for the Care and Use of Laboratory Animals published by the National Institutes of Health. All procedures were reviewed and approved by the University at Buffalo Institutional Animal Care and Use Committee (IACUC), approval number MIC33018Y. All work with human donors was approved by the University at Buffalo Human investigation Review Board (IRB), approval number STUDY00007111.

Data Availability

All data presented within this manuscript are found in the supportive data values file and available from the corresponding author upon request.

Author Contributions

EYIT conducted research, acquired data, analyzed data, and wrote the manuscript. AB conducted research, acquired data, and analyzed data. AYK, EL, MB, MC conducted research and acquired data. EAW provided materials. ENBG designed the research studies, wrote, and edited the manuscript, and had responsibility for final content. All authors read and approved the manuscript.

Funding Support

This work was supported by National Institute of Health grant R01 AG068568-01A1 to ENBG, Mark Diamond Research Funds to EYIT, and an AHA predoctoral fellowship to AB. The content is solely the responsibility of the authors and does not necessarily represent the official views of the National Institutes of Health.

746 **References**

747 1. Simmons SR, Bhalla M, Herring SE, Tchalla EYI, and Bou Ghanem EN. Older but
748 not wiser: The age-driven changes in neutrophil responses during pulmonary
749 infections. *Infect Immun.* 2021.

750 2. Mantovani A, Cassatella MA, Costantini C, and Jaillon S. Neutrophils in the
751 activation and regulation of innate and adaptive immunity. *Nature reviews*
752 *Immunology.* 2011;11(8):519-31.

753 3. Bert S, Nadkarni S, and Perretti M. Neutrophil-T cell crosstalk and the control of
754 the host inflammatory response. *Immunol Rev.* 2023;314(1):36-49.

755 4. Li Y, Wang W, Yang F, Xu Y, Feng C, and Zhao Y. The regulatory roles of
756 neutrophils in adaptive immunity. *Cell Communication and Signaling.* 2019;17(1).

757 5. Leliefeld PHC, Koenderman L, and Pillay J. How Neutrophils Shape Adaptive
758 Immune Responses. *Frontiers in Immunology.* 2015;6.

759 6. Shafqat A, Khan JA, Alkachem AY, Sabur H, Alkattan K, Yaqinuddin A, et al. How
760 Neutrophils Shape the Immune Response: Reassessing Their Multifaceted Role
761 in Health and Disease. *Int J Mol Sci.* 2023;24(24).

762 7. Abi Abdallah DS, Egan CE, Butcher BA, and Denkers EY. Mouse neutrophils are
763 professional antigen-presenting cells programmed to instruct Th1 and Th17 T-cell
764 differentiation. *International immunology.* 2011;23(5):317-26.

765 8. Culshaw S, Millington OR, Brewer JM, and McInnes IB. Murine neutrophils present
766 Class II restricted antigen. *Immunol Lett.* 2008;118(1):49-54.

767 9. Vono M, Lin A, Norrby-Teglund A, Koup RA, Liang F, and Lore K. Neutrophils
768 acquire the capacity for antigen presentation to memory CD4(+) T cells in vitro and
769 ex vivo. *Blood.* 2017;129(14):1991-2001.

770 10. Matsushima H, Geng S, Lu R, Okamoto T, Yao Y, Mayuzumi N, et al. Neutrophil
771 differentiation into a unique hybrid population exhibiting dual phenotype and
772 functionality of neutrophils and dendritic cells. *Blood.* 2013;121(10):1677-89.
773 11. de Kleijn S, Langereis JD, Leentjens J, Kox M, Netea MG, Koenderman L, et al.
774 IFN-γ-stimulated neutrophils suppress lymphocyte proliferation through
775 expression of PD-L1. *PLoS One.* 2013;8(8):e72249.
776 12. Kasten KR, Muenzer JT, and Caldwell CC. Neutrophils are significant producers
777 of IL-10 during sepsis. *Biochemical and Biophysical Research Communications.*
778 2010;393(1):28-31.
779 13. Pillay J, Kamp VM, Van Hoffen E, Visser T, Tak T, Lammers J-W, et al. A subset
780 of neutrophils in human systemic inflammation inhibits T cell responses through
781 Mac-1. *Journal of Clinical Investigation.* 2012;122(1):327-36.
782 14. Schmielau J, and Finn OJ. Activated granulocytes and granulocyte-derived
783 hydrogen peroxide are the underlying mechanism of suppression of t-cell function
784 in advanced cancer patients. *Cancer research.* 2001;61(12):4756-60.
785 15. Sangaletti S, Talarico G, Chiodoni C, Cappetti B, Botti L, Portararo P, et al. SPARC
786 Is a New Myeloid-Derived Suppressor Cell Marker Licensing Suppressive
787 Activities. *Front Immunol.* 2019;10:1369.
788 16. Jiang X, Wu X, Xiao Y, Wang P, Zheng J, Wu X, et al. The ectonucleotidases CD39
789 and CD73 on T cells: The new pillar of hematological malignancy. *Front Immunol.*
790 2023;14:1110325.
791 17. Allard B, Longhi MS, Robson SC, and Stagg J. The ectonucleotidases CD39 and
792 CD73: Novel checkpoint inhibitor targets. *Immunol Rev.* 2017;276(1):121-44.

793 18. Jee J, Bonnegarde-Bernard A, Duverger A, Iwakura Y, Cormet-Boyaka E, Martin
794 TL, et al. Neutrophils negatively regulate induction of mucosal IgA responses after
795 sublingual immunization. *Mucosal Immunol.* 2015;8(4):735-45.
796 19. Kamenyeva O, Boularan C, Kabat J, Cheung GYC, Cicala C, Yeh AJ, et al.
797 Neutrophil Recruitment to Lymph Nodes Limits Local Humoral Response to
798 Staphylococcus aureus. *PLoS pathogens.* 2015;11(4):e1004827.
799 20. Bird AK, Chang M, Barnard J, Goldman BI, Meednu N, Rangel-Moreno J, et al.
800 Neutrophils Slow Disease Progression in Murine Lupus via Modulation of
801 Autoreactive Germinal Centers. *The Journal of Immunology.* 2017;199(2):458-66.
802 21. Puga I, Cols M, Barra CM, He B, Cassis L, Gentile M, et al. B cell-helper
803 neutrophils stimulate the diversification and production of immunoglobulin in the
804 marginal zone of the spleen. *Nature immunology.* 2011;13(2):170-80.
805 22. Chorny A, Casas-Recasens S, Sintes J, Shan M, Polentarutti N, Garcia-Escudero
806 R, et al. The soluble pattern recognition receptor PTX3 links humoral innate and
807 adaptive immune responses by helping marginal zone B cells. *The Journal of*
808 *experimental medicine.* 2016;213(10):2167-85.
809 23. Musich T, Rahman MA, Mohanram V, Miller-Novak L, Demberg T, Venzon DJ, et
810 al. Neutrophil Vaccination Dynamics and Their Capacity To Mediate B Cell Help in
811 Rhesus Macaques. *Journal of immunology.* 2018;201(8):2287-302.
812 24. Bhattacharya P, Dey R, Saxena A, Karmakar S, Ismail N, Gannavaram S, et al.
813 Essential Role of Neutrophils in the Protective Immune Response Induced by a
814 Live Attenuated Leishmania Vaccine. *Journal of immunology.* 2020;205(12):3333-
815 47.

816 25. Trentini MM, de Oliveira FM, Kipnis A, and Junqueira-Kipnis AP. The Role of
817 Neutrophils in the Induction of Specific Th1 and Th17 during Vaccination against
818 Tuberculosis. *Front Microbiol.* 2016;7:898.
819 26. Tchalla EYI, Bhalla M, Wohlfert EA, and Bou Ghanem EN. Neutrophils Are
820 Required During Immunization With the Pneumococcal Conjugate Vaccine for
821 Protective Antibody Responses and Host Defense Against Infection. *J Infect Dis.*
822 2020;222(8):1363-70.
823 27. CDC. Center for Disease Control and Prevention. Active Bacterial Core
824 Surveillance Report, Emerging Infections Program Network, Streptococcus
825 pneumoniae. 2022.
826 28. Vinuesa CG, Linterman MA, Yu D, and MacLennan IC. Follicular Helper T Cells.
827 *Annual review of immunology.* 2016;34:335-68.
828 29. Rappuoli R. Glycoconjugate vaccines: Principles and mechanisms. *Sci Transl*
829 *Med.* 2018;10(456).
830 30. Sterrett S, Peng BJ, Burton RL, LaFon DC, Westfall AO, Singh S, et al. Peripheral
831 CD4 T follicular cells induced by a conjugated pneumococcal vaccine correlate
832 with enhanced opsonophagocytic antibody responses in younger individuals.
833 *Vaccine.* 2020.
834 31. De Silva NS, and Klein U. Dynamics of B cells in germinal centres. *Nature reviews*
835 *Immunology.* 2015;15(3):137-48.
836 32. Pollard AJ, Perrett KP, and Beverley PC. Maintaining protection against invasive
837 bacteria with protein–polysaccharide conjugate vaccines. *Nature Reviews*
838 *Immunology.* 2009;9(3):213-20.

839 33. Rappuoli R, De Gregorio E, and Costantino P. On the mechanisms of conjugate
840 vaccines. *Proceedings of the National Academy of Sciences.* 2019;116(1):14-6.
841 34. Murphy KM, Weaver C, Mowat A, Berg L, Chaplin D, Janeway CA, et al. *Janeway's*
842 *immunobiology.* 2017.
843 35. Rappuoli R, De Gregorio E, and Costantino P. On the mechanisms of conjugate
844 vaccines. *Proc Natl Acad Sci U S A.* 2019;116(1):14-6.
845 36. Vidarsson G, Dekkers G, and Rispens T. IgG Subclasses and Allotypes: From
846 Structure to Effector Functions. *Frontiers in Immunology.* 2014;5(520).
847 37. Forthal DN. Functions of Antibodies. *Microbiol Spectr.* 2014;2(4):1-17.
848 38. Dong C. Cytokine Regulation and Function in T Cells. *Annual review of*
849 *immunology.* 2021;39(1):51-76.
850 39. Vazquez MI, Catalan-Dibene J, and Zlotnik A. B cells responses and cytokine
851 production are regulated by their immune microenvironment. *Cytokine.*
852 2015;74(2):318-26.
853 40. Shevyrev D, and Tereshchenko V. Treg Heterogeneity, Function, and
854 Homeostasis. *Front Immunol.* 2019;10:3100.
855 41. Ndure J, and Flanagan KL. Targeting regulatory T cells to improve vaccine
856 immunogenicity in early life. *Front Microbiol.* 2014;5:477.
857 42. Bayry J. Regulatory T cells as adjuvant target for enhancing the viral disease
858 vaccine efficacy. *Virusdisease.* 2014;25(1):18-25.
859 43. Moore AC, Gallimore A, Draper SJ, Watkins KR, Gilbert SC, and Hill AV. Anti-
860 CD25 antibody enhancement of vaccine-induced immunogenicity: increased

861 durable cellular immunity with reduced immunodominance. *Journal of*
862 *immunology.* 2005;175(11):7264-73.
863 44. Pere H, Tanchot C, Bayry J, Terme M, Taieb J, Badoual C, et al. Comprehensive
864 analysis of current approaches to inhibit regulatory T cells in cancer.
865 *Oncoimmunology.* 2012;1(3):326-33.
866 45. Weingartner E, and Golding A. Direct control of B cells by Tregs: An opportunity
867 for long-term modulation of the humoral response. *Cell Immunol.* 2017;318:8-16.
868 46. Stepkowski S, Bekbolsynov D, Oenick J, Brar S, Mierzejewska B, Rees MA, et al.
869 The Major Role of T Regulatory Cells in the Efficiency of Vaccination in General
870 and Immunocompromised Populations: A Review. *Vaccines (Basel).* 2024;12(9).
871 47. Togashi Y, Shitara K, and Nishikawa H. Regulatory T cells in cancer
872 immunosuppression - implications for anticancer therapy. *Nat Rev Clin Oncol.*
873 2019;16(6):356-71.
874 48. Brezar V, Ruffin N, Richert L, Surenaud M, Lacabaratz C, Palucka K, et al.
875 Decreased HIV-specific T-regulatory responses are associated with effective DC-
876 vaccine induced immunity. *PLoS pathogens.* 2015;11(3):e1004752.
877 49. Boudewijns M, Jeurissen A, Wuyts M, Moens L, Boon L, Van Neerven JJ, et al.
878 Blockade of CTLA-4 (CD152) enhances the murine antibody response to
879 pneumococcal capsular polysaccharides. *J Leukoc Biol.* 2005;78(5):1060-9.
880 50. He SWJ, van de Garde MDB, Pieren DKJ, Poelen MCM, Voss F, Abdullah MR, et
881 al. Diminished Pneumococcal-Specific CD4(+) T-Cell Response is Associated
882 With Increased Regulatory T Cells at Older Age. *Front Aging.* 2021;2:746295.

883 51. Maceiras AR, Fonseca VR, Agua-Doce A, and Graca L. T follicular regulatory cells
884 in mice and men. *Immunology.* 2017;152(1):25-35.
885 52. Lu Y, and Craft J. T Follicular Regulatory Cells: Choreographers of Productive
886 Germinal Center Responses. *Front Immunol.* 2021;12:679909.
887 53. Qi J, Liu C, Bai Z, Li X, and Yao G. T follicular helper cells and T follicular regulatory
888 cells in autoimmune diseases. *Front Immunol.* 2023;14:1178792.
889 54. Sage PT, Ron-Harel N, Juneja VR, Sen DR, Maleri S, Sungnak W, et al.
890 Suppression by T(FR) cells leads to durable and selective inhibition of B cell
891 effector function. *Nature immunology.* 2016;17(12):1436-46.
892 55. Xie MM, Chen Q, Liu H, Yang K, Koh B, Wu H, et al. T follicular regulatory cells
893 and IL-10 promote food antigen-specific IgE. *J Clin Invest.* 2020;130(7):3820-32.
894 56. Jacobsen JT, Hu W, TB RC, Solem S, Galante A, Lin Z, et al. Expression of Foxp3
895 by T follicular helper cells in end-stage germinal centers. *Science.* 2021;373(6552).
896 57. Himmel ME, Crome SQ, Ivison S, Piccirillo C, Steiner TS, and Levings MK. Human
897 CD4+ FOXP3+ regulatory T cells produce CXCL8 and recruit neutrophils.
898 *European journal of immunology.* 2011;41(2):306-12.
899 58. Richards H, Williams A, Jones E, Hindley J, Godkin A, Simon AK, et al. Novel role
900 of regulatory T cells in limiting early neutrophil responses in skin. *Immunology.*
901 2010;131(4):583-92.
902 59. Lewkowicz N, Klink M, Mycko MP, and Lewkowicz P. Neutrophil--CD4+CD25+ T
903 regulatory cell interactions: a possible new mechanism of infectious tolerance.
904 *Immunobiology.* 2013;218(4):455-64.

905 60. Mishalian I, Bayuh R, Eruslanov E, Michaeli J, Levy L, Zolotarov L, et al.
906 Neutrophils recruit regulatory T-cells into tumors via secretion of CCL17--a new
907 mechanism of impaired antitumor immunity. *Int J Cancer.* 2014;135(5):1178-86.
908 61. Perobelli SM, Mercadante AC, Galvani RG, Goncalves-Silva T, Alves AP, Pereira-
909 Neves A, et al. G-CSF-Induced Suppressor IL-10+ Neutrophils Promote
910 Regulatory T Cells That Inhibit Graft-Versus-Host Disease in a Long-Lasting and
911 Specific Way. *Journal of immunology.* 2016;197(9):3725-34.
912 62. Nadkarni S, Smith J, Sferruzzi-Perri AN, Ledwozyw A, Kishore M, Haas R, et al.
913 Neutrophils induce proangiogenic T cells with a regulatory phenotype in
914 pregnancy. *Proc Natl Acad Sci U S A.* 2016;113(52):E8415-E24.
915 63. Gao Y, Min K, Zhang Y, Su J, Greenwood M, and Gronert K. Female-Specific
916 Downregulation of Tissue Polymorphonuclear Neutrophils Drives Impaired
917 Regulatory T Cell and Amplified Effector T Cell Responses in Autoimmune Dry
918 Eye Disease. *Journal of immunology.* 2015;195(7):3086-99.
919 64. Wagenvoort GH, Sanders EA, Vlaminckx BJ, de Melker HE, van der Ende A, and
920 Knol MJ. Sex differences in invasive pneumococcal disease and the impact of
921 pneumococcal conjugate vaccination in the Netherlands, 2004 to 2015. *Euro*
922 *Surveill.* 2017;22(10).
923 65. Wiese AD, Grijalva CG, Zhu Y, Mitchel EF, Jr., and Griffin MR. Changes in
924 Childhood Pneumonia Hospitalizations by Race and Sex Associated with
925 Pneumococcal Conjugate Vaccines. *Emerg Infect Dis.* 2016;22(6).

926 66. Soneji S, and Metlay J. Mortality reductions for older adults differ by race/ethnicity
927 and gender since the introduction of adult and pediatric pneumococcal vaccines.
928 *Public Health Rep.* 2011;126(2):259-69.
929 67. Tchalla EYI, Betadpur A, Khalil AY, Bhalla M, and Bou Ghanem EN. Sex-based
930 difference in immune responses and efficacy of the pneumococcal conjugate
931 vaccine. *J Leukoc Biol.* 2024.
932 68. Beauvillain C, Cunin P, Doni A, Scotet M, Jaillon S, Loiry ML, et al. CCR7 is
933 involved in the migration of neutrophils to lymph nodes. *Blood.* 2011;117(4):1196-
934 204.
935 69. Hampton HR, Bailey J, Tomura M, Brink R, and Chtanova T. Microbe-dependent
936 lymphatic migration of neutrophils modulates lymphocyte proliferation in lymph
937 nodes. *Nat Commun.* 2015;6:7139.
938 70. Stavnezer J, Guikema JE, and Schrader CE. Mechanism and regulation of class
939 switch recombination. *Annual review of immunology.* 2008;26:261-92.
940 71. Di Noia JM, and Neuberger MS. Molecular mechanisms of antibody somatic
941 hypermutation. *Annu Rev Biochem.* 2007;76:1-22.
942 72. Morel C, Badell E, Abadie V, Robledo M, Setterblad N, Gluckman JC, et al.
943 Mycobacterium bovis BCG-infected neutrophils and dendritic cells cooperate to
944 induce specific T cell responses in humans and mice. *European journal of*
945 *immunology.* 2008;38(2):437-47.
946 73. Abbas AK, Burstein HJ, and Bogen SA. Determinants of helper T cell-dependent
947 antibody production. *Semin Immunol.* 1993;5(6):441-7.

948 74. Karachunski PI, Ostlie NS, Monfardini C, and Conti-Fine BM. Absence of IFN-γ or
949 IL-12 Has Different Effects on Experimental Myasthenia Gravis in C57BL/6 Mice.
950 *The Journal of Immunology.* 2000;164(10):5236-44.
951 75. Ballesteros I, Rubio-Ponce A, Genua M, Lusito E, Kwok I, Fernandez-Calvo G, et
952 al. Co-option of Neutrophil Fates by Tissue Environments. *Cell.* 2020;183(5):1282-
953 97 e18.
954 76. Yang P, Li Y, Xie Y, and Liu Y. Different Faces for Different Places: Heterogeneity
955 of Neutrophil Phenotype and Function. *J Immunol Res.* 2019;2019:8016254.
956 77. Rambault M, Doz-Deblauwe E, Le Vern Y, Carreras F, Cunha P, Germon P, et al.
957 Neutrophils Encompass a Regulatory Subset Suppressing T Cells in Apparently
958 Healthy Cattle and Mice. *Front Immunol.* 2021;12:625244.
959 78. Christiaansen AF, Dixit UG, Coler RN, Marie Beckmann A, Reed SG, Winokur PL,
960 et al. CD11a and CD49d enhance the detection of antigen-specific T cells following
961 human vaccination. *Vaccine.* 2017;35(33):4255-61.
962 79. Liu S, Ren J, and Ten Dijke P. Targeting TGFβ signal transduction for cancer
963 therapy. *Signal Transduction and Targeted Therapy.* 2021;6(1).
964 80. Areström I, Zuber B, Bengtsson T, and Ahlborg N. Measurement of human latent
965 Transforming Growth Factor-β1 using a latency associated protein-reactive ELISA.
966 *J Immunol Methods.* 2012;379(1-2):23-9.
967 81. Farkas AM, Marvel DM, and Finn OJ. Antigen choice determines vaccine-induced
968 generation of immunogenic versus tolerogenic dendritic cells that are marked by
969 differential expression of pancreatic enzymes. *Journal of immunology.*
970 2013;190(7):3319-27.

971 82. Jin RM, Blair SJ, Warunek J, Heffner RR, Blader IJ, and Wohlfert EA. Regulatory
972 T Cells Promote Myositis and Muscle Damage in Toxoplasma gondii Infection.
973 *Journal of immunology.* 2017;198(1):352-62.
974 83. Lahl K, Loddenkemper C, Drouin C, Freyer J, Arnason J, Eberl G, et al. Selective
975 depletion of Foxp3+ regulatory T cells induces a scurfy-like disease. *The Journal*
976 *of experimental medicine.* 2007;204(1):57-63.
977 84. Nauseef WM. Human neutrophils ≠ murine neutrophils: Does it matter? *Immunol*
978 *Rev.* 2023;314(1):442-56.
979 85. Fontenot JD, Gavin MA, and Rudensky AY. Foxp3 programs the development and
980 function of CD4+CD25+ regulatory T cells. *Nature immunology.* 2003;4(4):330-6.
981 86. Ono M. Control of regulatory T-cell differentiation and function by T-cell receptor
982 signalling and Foxp3 transcription factor complexes. *Immunology.* 2020;160(1):24-
983 37.
984 87. Bank U, Reinhold D, Schneemilch C, Kunz D, Synowitz HJ, and Ansorge S.
985 Selective proteolytic cleavage of IL-2 receptor and IL-6 receptor ligand binding
986 chains by neutrophil-derived serine proteases at foci of inflammation. *Journal of*
987 *interferon & cytokine research : the official journal of the International Society for*
988 *Interferon and Cytokine Research.* 1999;19(11):1277-87.
989 88. Harris F, Berdugo YA, and Tree T. IL-2-based approaches to Treg enhancement.
990 *Clinical and experimental immunology.* 2023;211(2):149-63.
991 89. Ariel A, Yavin EJ, Hershkoviz R, Avron A, Franitza S, Hardan I, et al. IL-2 induces
992 T cell adherence to extracellular matrix: inhibition of adherence and migration by

993 IL-2 peptides generated by leukocyte elastase. *Journal of immunology.*
994 1998;161(5):2465-72.
995 90. Fu Z, Akula S, Thorpe M, and Hellman L. Potent and Broad but not Unselective
996 Cleavage of Cytokines and Chemokines by Human Neutrophil Elastase and
997 Proteinase 3. *Int J Mol Sci.* 2020;21(2).
998 91. Chen W. TGF-beta Regulation of T Cells. *Annual review of immunology.*
999 2023;41:483-512.
1000 92. Kretschmer K, Apostolou I, Hawiger D, Khazaie K, Nussenzweig MC, and von
1001 Boehmer H. Inducing and expanding regulatory T cell populations by foreign
1002 antigen. *Nature immunology.* 2005;6(12):1219-27.
1003 93. Corse E, Gottschalk RA, and Allison JP. Strength of TCR-peptide/MHC
1004 interactions and in vivo T cell responses. *Journal of immunology.*
1005 2011;186(9):5039-45.
1006 94. Ohkura N, Hamaguchi M, and Sakaguchi S. FOXP3+ regulatory T cells: control of
1007 FOXP3 expression by pharmacological agents. *Trends Pharmacol Sci.*
1008 2011;32(3):158-66.
1009 95. Stream A, Corriden R, Dohrmann S, Gallo RL, Nizet V, and Anderson EL. The
1010 Effect of Retinoic Acid on Neutrophil Innate Immune Interactions With Cutaneous
1011 Bacterial Pathogens. *Infect Microbes Dis.* 2024;6(2):65-73.
1012 96. Mader JS, Ewen C, Hancock RE, and Bleackley RC. The human cathelicidin, LL-
1013 37, induces granzyme-mediated apoptosis in regulatory T cells. *J Immunother.*
1014 2011;34(3):229-35.

1015 97. Glemain A, Neel M, Neel A, Andre-Gregoire G, Gavard J, Martinet B, et al.
1016 Neutrophil-derived extracellular vesicles induce endothelial inflammation and
1017 damage through the transfer of miRNAs. *J Autoimmun.* 2022;129:102826.
1018 98. Gomez I, Ward B, Souilhol C, Recarti C, Ariaans M, Johnston J, et al. Neutrophil
1019 microvesicles drive atherosclerosis by delivering miR-155 to atheroprone
1020 endothelium. *Nat Commun.* 2020;11(1):214.
1021 99. Jiao Y, Zhang T, Zhang C, Ji H, Tong X, Xia R, et al. Exosomal miR-30d-5p of
1022 neutrophils induces M1 macrophage polarization and primes macrophage
1023 pyroptosis in sepsis-related acute lung injury. *Crit Care.* 2021;25(1):356.
1024 100. Lu J, Wang W, Li P, Wang X, Gao C, Zhang B, et al. MiR-146a regulates regulatory
1025 T cells to suppress heart transplant rejection in mice. *Cell Death Discov.*
1026 2021;7(1):165.
1027 101. Kunze-Schumacher H, and Krueger A. The Role of MicroRNAs in Development
1028 and Function of Regulatory T Cells - Lessons for a Better Understanding of
1029 MicroRNA Biology. *Front Immunol.* 2020;11:2185.
1030 102. Arroyo AB, Fernandez-Perez MP, Del Monte A, Aguila S, Mendez R, Hernandez-
1031 Antolin R, et al. miR-146a is a pivotal regulator of neutrophil extracellular trap
1032 formation promoting thrombosis. *Haematologica.* 2021;106(6):1636-46.
1033 103. Garley M, Nowak K, and Jablonska E. Neutrophil microRNAs. *Biol Rev Camb*
1034 *Philos Soc.* 2024;99(3):864-77.
1035 104. Toka FN, Suvas S, and Rouse BT. CD4+ CD25+ T cells regulate vaccine-
1036 generated primary and memory CD8+ T-cell responses against herpes simplex
1037 virus type 1. *J Virol.* 2004;78(23):13082-9.

1038 105. Levy Y, Thiebaut R, Montes M, Lacabaratz C, Sloan L, King B, et al. Dendritic cell-
1039 based therapeutic vaccine elicits polyfunctional HIV-specific T-cell immunity
1040 associated with control of viral load. *European journal of immunology.*
1041 2014;44(9):2802-10.
1042 106. Wang P, and Zheng SG. Regulatory T cells and B cells: implication on autoimmune
1043 diseases. *Int J Clin Exp Pathol.* 2013;6(12):2668-74.
1044 107. Gonzalez-Figueroa P, Roco JA, Papa I, Nunez Villacis L, Stanley M, Linterman
1045 MA, et al. Follicular regulatory T cells produce neuritin to regulate B cells. *Cell.*
1046 2021;184(7):1775-89 e19.
1047 108. Tan D, Yin W, Guan F, Zeng W, Lee P, Candotti F, et al. B cell-T cell interplay in
1048 immune regulation: A focus on follicular regulatory T and regulatory B cell
1049 functions. *Front Cell Dev Biol.* 2022;10:991840.
1050 109. Lim HW, Hillsamer P, Banham AH, and Kim CH. Cutting edge: direct suppression
1051 of B cells by CD4+ CD25+ regulatory T cells. *Journal of immunology.*
1052 2005;175(7):4180-3.
1053 110. Park SR. Activation-induced Cytidine Deaminase in B Cell Immunity and Cancers.
1054 *Immune Netw.* 2012;12(6):230-9.
1055 111. McBride KM, Gazumyan A, Woo EM, Schwickert TA, Chait BT, and Nussenzweig
1056 MC. Regulation of class switch recombination and somatic mutation by AID
1057 phosphorylation. *The Journal of experimental medicine.* 2008;205(11):2585-94.
1058 112. Chaudhuri J, Khuong C, and Alt FW. Replication protein A interacts with AID to
1059 promote deamination of somatic hypermutation targets. *Nature.*
1060 2004;430(7003):992-8.

1061 113. Basu U, Chaudhuri J, Alpert C, Dutt S, Ranganath S, Li G, et al. The AID antibody
1062 diversification enzyme is regulated by protein kinase A phosphorylation. *Nature.*
1063 2005;438(7067):508-11.
1064 114. Demorest ZL, Li M, and Harris RS. Phosphorylation directly regulates the intrinsic
1065 DNA cytidine deaminase activity of activation-induced deaminase and
1066 APOBEC3G protein. *J Biol Chem.* 2011;286(30):26568-75.
1067 115. Gazumyan A, Timachova K, Yuen G, Siden E, Di Virgilio M, Woo EM, et al. Amino-
1068 terminal phosphorylation of activation-induced cytidine deaminase suppresses c-
1069 myc/IgH translocation. *Mol Cell Biol.* 2011;31(3):442-9.
1070 116. Klein M, and Bopp T. Cyclic AMP Represents a Crucial Component of Treg Cell-
1071 Mediated Immune Regulation. *Front Immunol.* 2016;7:315.
1072 117. Wiemken TL, Carrico RM, Klein SL, Jonsson CB, Peyrani P, Kelley RR, et al. The
1073 effectiveness of the polysaccharide pneumococcal vaccine for the prevention of
1074 hospitalizations due to Streptococcus pneumoniae community-acquired
1075 pneumonia in the elderly differs between the sexes: results from the Community-
1076 Acquired Pneumonia Organization (CAPO) international cohort study. *Vaccine.*
1077 2014;32(19):2198-203.
1078 118. Robinson GA, Peng J, Peckham H, Butler G, Pineda-Torra I, Ciurtin C, et al.
1079 Investigating sex differences in T regulatory cells from cisgender and transgender
1080 healthy individuals and patients with autoimmune inflammatory disease: a cross-
1081 sectional study. *Lancet Rheumatol.* 2022;4(10):e710-e24.

1082 119. Afshan G, Afzal N, and Qureshi S. CD4+CD25(hi) regulatory T cells in healthy
1083 males and females mediate gender difference in the prevalence of autoimmune
1084 diseases. *Clin Lab.* 2012;58(5-6):567-71.
1085 120. Raynor J, Lages CS, Shehata H, Hildeman DA, and Chougnet CA. Homeostasis
1086 and function of regulatory T cells in aging. *Curr Opin Immunol.* 2012;24(4):482-7.
1087 121. Flanagan KL, Fink AL, Plebanski M, and Klein SL. Sex and Gender Differences in
1088 the Outcomes of Vaccination over the Life Course. *Annu Rev Cell Dev Biol.*
1089 2017;33:577-99.
1090 122. Pollard AJ, and Bijker EM. A guide to vaccinology: from basic principles to new
1091 developments. *Nature Reviews Immunology.* 2021;21(2):83-100.
1092 123. de St Maurice A, Schaffner W, Griffin MR, Halasa N, and Grijalva CG. Persistent
1093 Sex Disparities in Invasive Pneumococcal Diseases in the Conjugate Vaccine Era.
1094 *J Infect Dis.* 2016;214(5):792-7.
1095 124. Bhalla M, Nayerhoda R, Tchalla EYI, Abamonte A, Park D, Simmons SR, et al.
1096 Liposomal Encapsulation of Polysaccharides (LEPS) as an Effective Vaccine
1097 Strategy to Protect Aged Hosts Against S. pneumoniae Infection. *Frontiers in*
1098 *Aging.* 2021;2.
1099 125. Bou Ghanem EN, Clark S, Roggensack SE, McIver SR, Alcaide P, Haydon PG, et
1100 al. Extracellular Adenosine Protects against Streptococcus pneumoniae Lung
1101 Infection by Regulating Pulmonary Neutrophil Recruitment. *PLoS Pathog.*
1102 2015;11(8):e1005126.
1103 126. Lenhard A, Joma BH, Siwapornchai N, Hakansson AP, Leong JM, and Bou
1104 Ghanem EN. A Mouse Model for the Transition of Streptococcus pneumoniae from

1105 Colonizer to Pathogen upon Viral Co-Infection Recapitulates Age-Exacerbated
1106 Illness. *J Vis Exp.* 2022(187).
1107 127. Casanova-Acebes M, Pitaval C, Weiss LA, Nombela-Arrieta C, Chèvre R, N AG,
1108 et al. Rhythmic modulation of the hematopoietic niche through neutrophil
1109 clearance. *Cell.* 2013;153(5):1025-35.
1110
1111
1112
1113
1114
1115
1116
1117
1118
1119
1120
1121
1122
1123
1124
1125
1126
1127
1128
1129

1130 **Figures and legends**

A. Migration markers expression on circulating PMNs

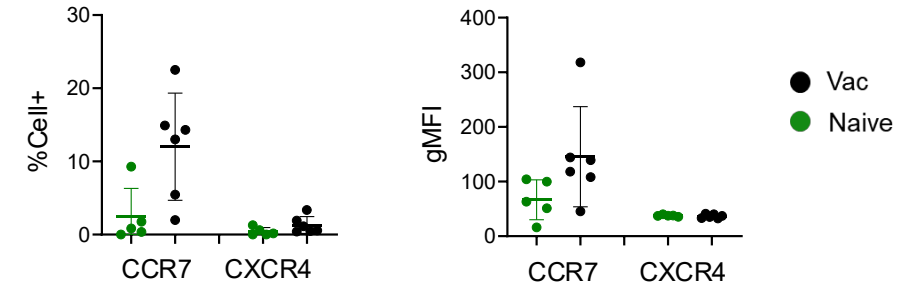

B. PMN influx

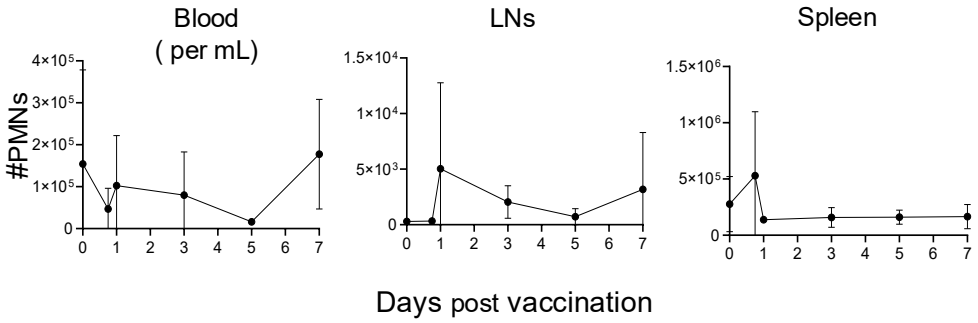

1131

1132 **Figure 1: PMN migration to secondary lymphoid organs following vaccination.** Adult
1133 C57BL/6 female mice were injected with PCV or PBS. (A) Blood was collected from the mice 24
1134 hours following vaccination and assessed using flow cytometry. Percentages (left) and gMFI
1135 (right) of CCR7 and CXCR4 on PMNs ($Ly6G^+CD11b^+$) were determined. (B) At different
1136 timepoints post vaccination, blood, spleen and vLNs were collected from all mice and PMN
1137 ($Ly6G^+CD11b^+$) numbers was assessed using flow cytometry. (A) Data are pooled from 3
1138 separate experiments and each dot represents an individual mouse with a total of n=5 naïve and
1139 n=6 vaccinated mice. Graphs represent the mean +/- SD. (B) Data are pooled from 3 separate
1140 experiments with a total of 6 mice per timepoint. Line graphs represent the mean +/- 95%
1141 confidence interval. Abbreviations: gMFI = geometric Mean Fluorescence Intensity.

1142

A. PMN depletion

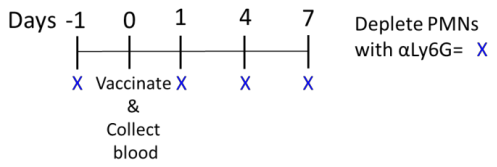

B. Tregs and PMN depletion

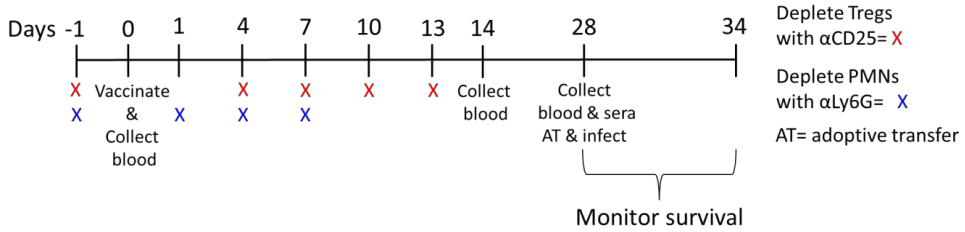

Figure 2: PMN and Treg depletion models. Adult C57BL/6 female mice were injected with PCV or PBS and depleted of their PMNs and/or Tregs or treated with isotype controls. (A) Depletion timeline of PMNs using an αLy6G antibody. (B) Depletion timeline of Tregs using an αCD25 antibody.

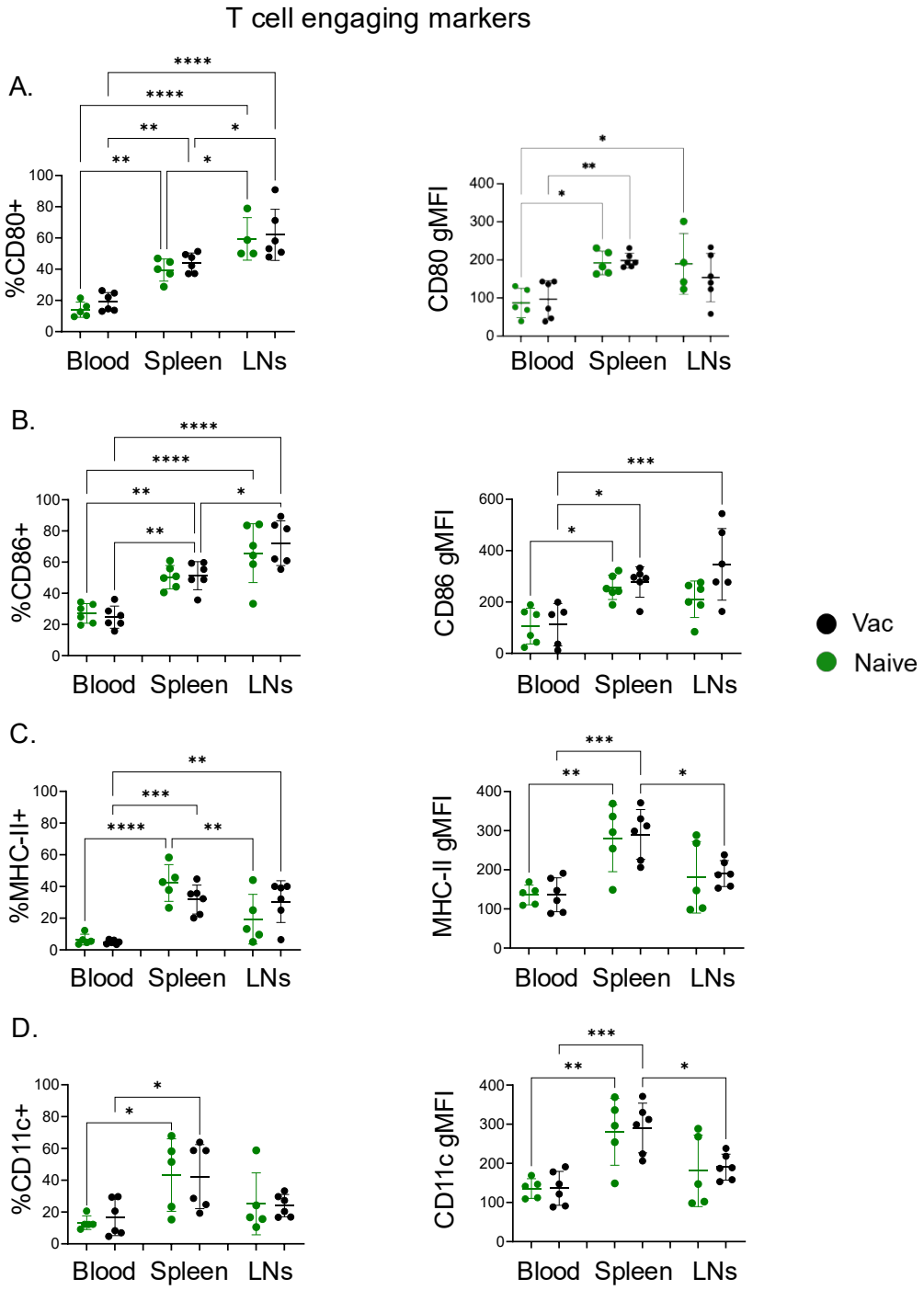

1159

1160 **Figure 3: PMN expression of T cell engaging markers following PCV vaccination.** Adult

1161 C57BL/6 female mice were injected with PCV or PBS. At 18- or 24 hours post vaccination,

1162 blood, spleen and vLNs were collected and assessed using flow cytometry. Percentages (left)

1163 and gMFI (right) of (A) CD80, (B) CD86, (C) MHC-II, and (D) CD11c on PMNs ($Ly6G^{+}CD11b^{+}$)

were determined. Data are pooled from 3 separate experiments and each dot represents an individual mouse with a total of n=5 naïve and n=6 vaccinated mice. * denotes significant differences between the indicated groups as determined by One-Way ANOVA followed by Šídák's multiple comparisons test. * is $p \leq 0.05$, ** is $p \leq 0.01$, *** is $p \leq 0.001$, and **** is $p \leq 0.0001$. Graphs represent the mean +/- SD. Abbreviations: gMFI = geometric Mean Fluorescence Intensity; MHC = Major Histocompatibility Complex.

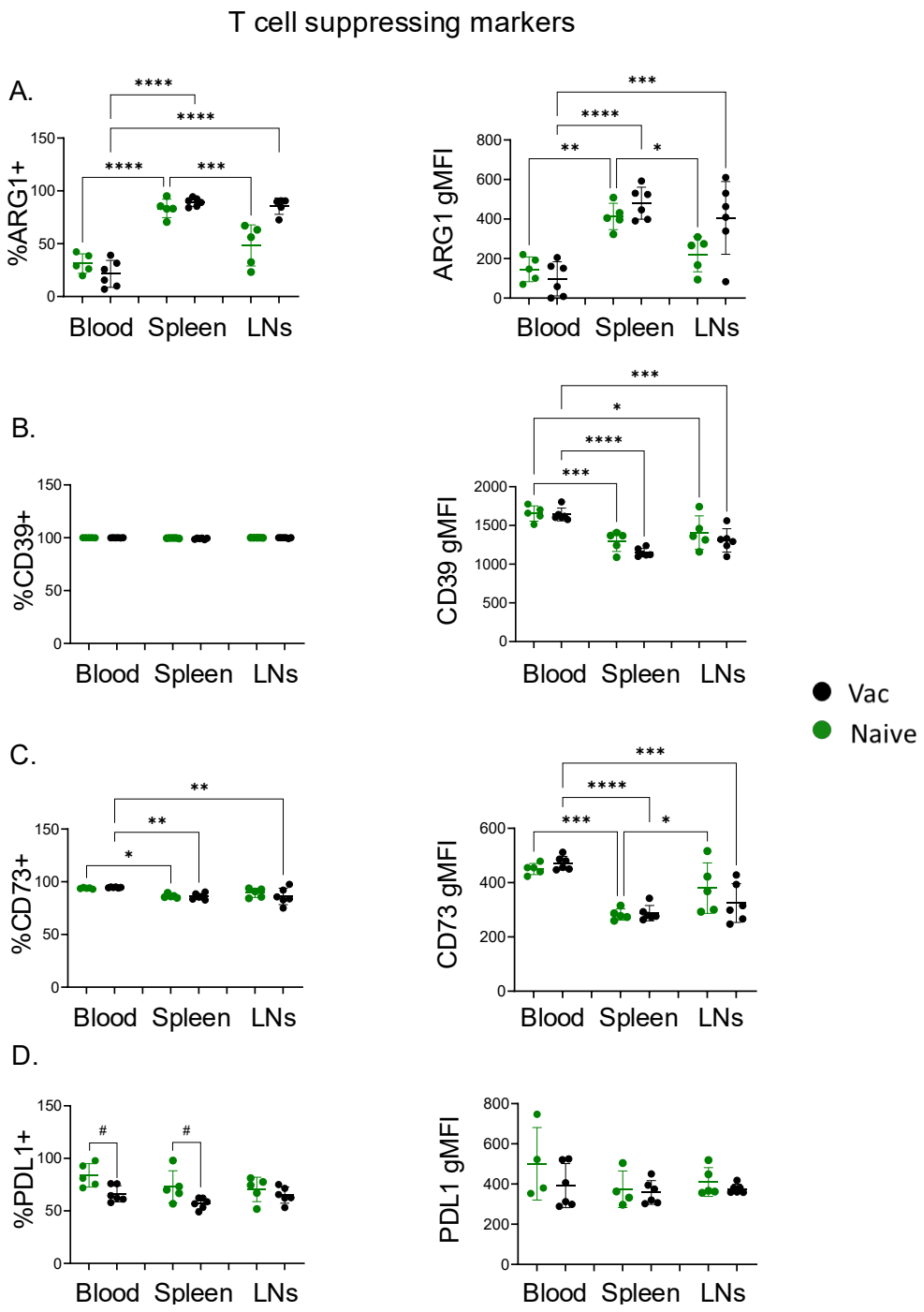

Figure 4: PMN expression of T cell suppressing markers following PCV vaccination. Adult C57BL/6 female mice were injected with PCV or PBS. At 18 hours post vaccination, blood, spleen and vLNs were collected and assessed using flow cytometry. Percentages (left) and gMFI (right) of (A) ARG1, (B) CD39, (C) CD73, and (D) PD-L1 on PMNs ($Ly6G^{+}CD11b^{+}$) were determined.

1179 Data are pooled from 3 separate experiments and each dot represents an individual mouse with
1180 a total of n=5 naïve and n=6 vaccinated mice. * denotes significant differences between the
1181 indicated groups as determined by One-Way ANOVA followed by Šídák's multiple comparisons
1182 test and # denotes significant differences between the indicated groups as determined by
1183 Student's t test. * and # is $p \leq 0.05$, ** is $p \leq 0.01$, *** is $p \leq 0.001$, and **** is $p \leq 0.0001$. Graphs
1184 represent the mean +/- SD. Abbreviations: gMFI = geometric Mean Fluorescence Intensity; ARG=
1185 arginase.
1186
1187
1188
1189
1190
1191
1192
1193
1194
1195
1196
1197

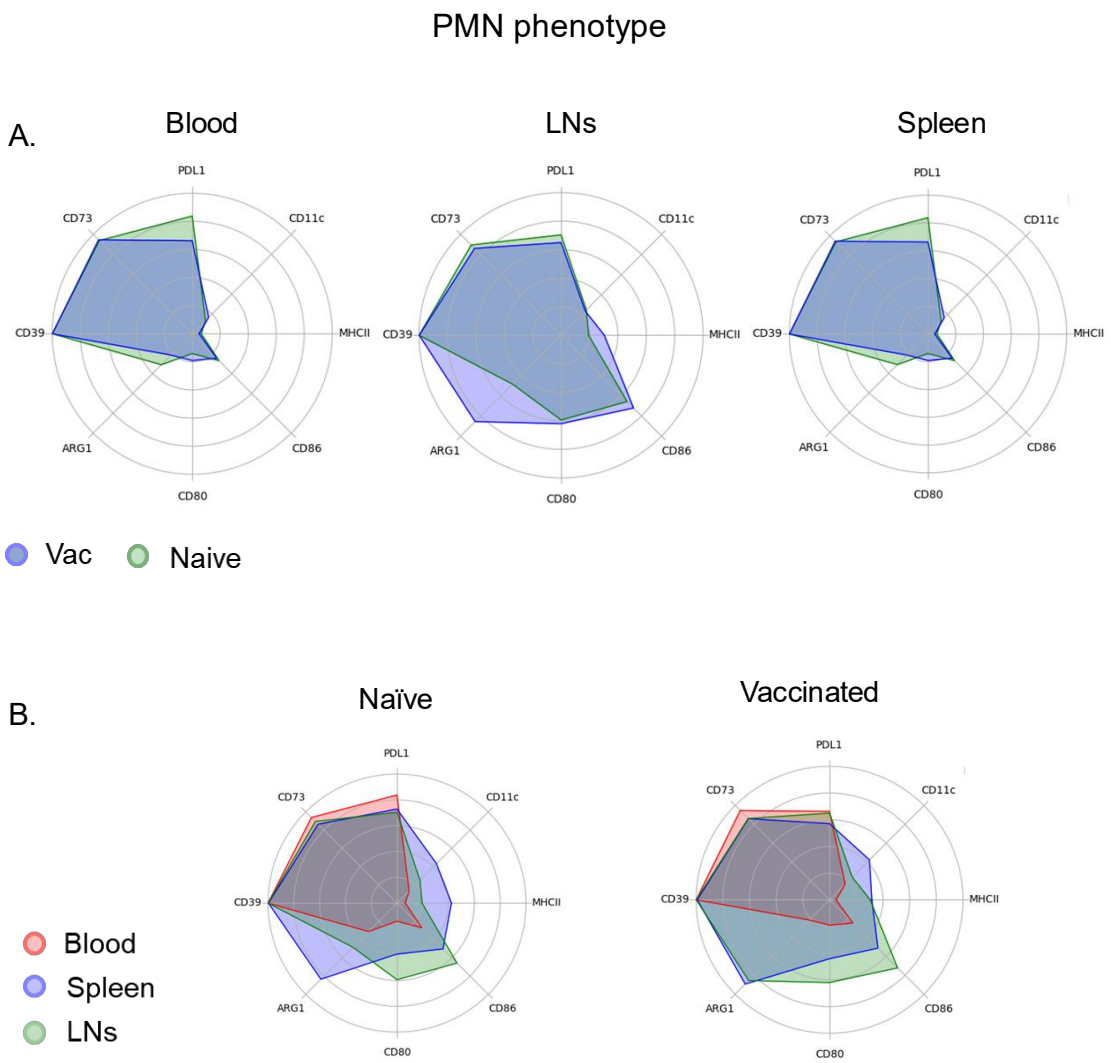

1198

1199 **Figure 5: PMN phenotype following PCV vaccination.** Adult C57BL/6 female mice were
1200 injected with PCV or PBS. (A). (B-C) At 18- or 24 hours post vaccination, blood, spleen and vLNs
1201 were collected and assessed using flow cytometry. Percent expressions of MHC-II, CD80, CD86,
1202 CD11c, PD-L1, ARG1, CD73 and CD39 on PMNs were determined. Data show percent
1203 expression of markers on PMNs from naïve and vaccinated mice overlayed for each tissue/organ
1204 (B) and PMNs in all organs/tissue overlayed for naïve and vaccinated mice (C). (A) (B-C) Data
1205 are pooled from 3 separate experiments with a total of n=5 naïve and n=6 vaccinated mice and
1206 are presented as radar plots generated using R studio.

1207

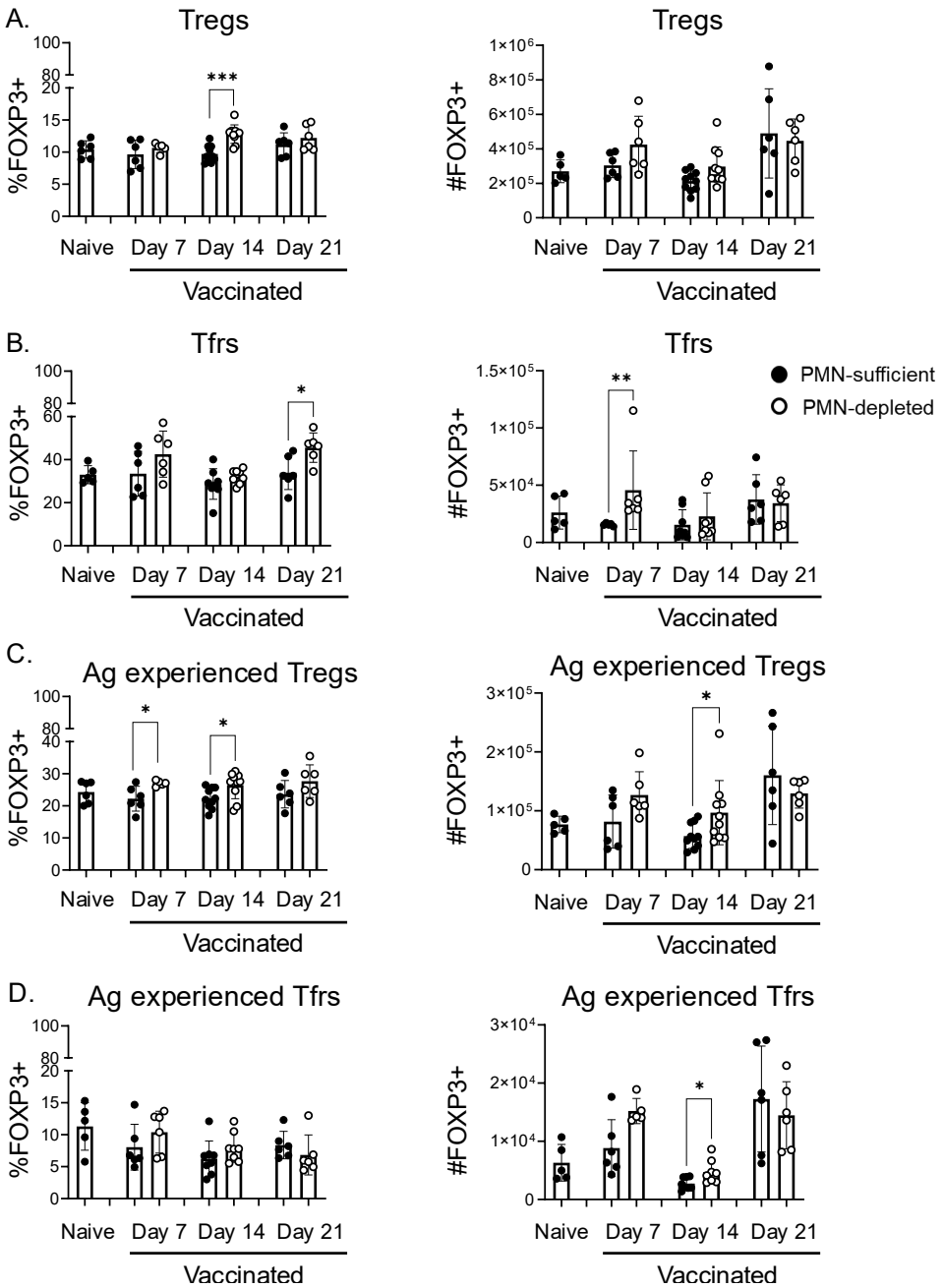

Figure 6: Effect of PMN depletion on regulatory T cells. Adult C57BL/6 female mice were injected with PCV or PBS and depleted of their PMNs or treated with an isotype control. Spleens were collected from all mice and assessed using flow cytometry on days 7, 14 and 21 post vaccination. (A-B) Total ($CD4^+TCR\beta^+$) and (C-D) antigen experienced ($CD11a^+CD49d^+$) T cells were gated on. Percentages (left) and numbers (right) of (A&C) regulatory T cells ($FOXP3^+$) and (B&D) T follicular regulatory T cells ($CXCR5^+PD1^+$ $FOXP3^+$) were determined. Data are pooled

1215 from 4 separate experiments and each dot represents an individual mouse with a total of n=6
1216 naïve, n=6 vaccinated day 7, n=8-10 vaccinated day 14, and n=6 vaccinated day 21 mice per
1217 group. * denotes significant differences between the indicated groups as determined by Mann-
1218 Whitney test. * is $p \leq 0.05$, ** is $p \leq 0.01$, and *** is $p \leq 0.001$. Bar graphs represent the mean +/- SD.
1219
1220
1221
1222
1223
1224
1225
1226
1227
1228
1229
1230
1231
1232
1233
1234

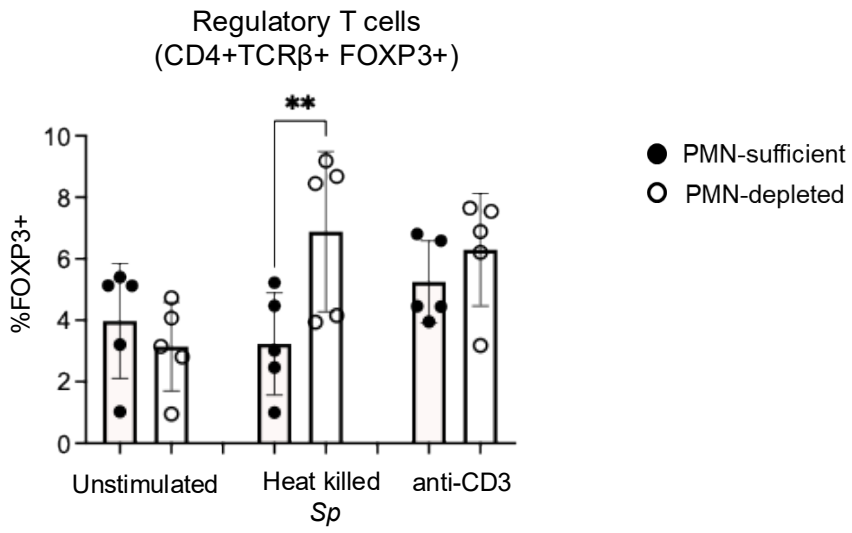

1235

1236 **Figure 7: Effect of PMN depletion on Tregs in mice *in vitro.*** Adult C57BL/6 female mice were
1237 injected with PCV or PBS and depleted of their PMNs or treated with an isotype control. On day
1238 1 post vaccination, splenocytes were isolated and cultured in the presence or absence of PMNs
1239 for 2 days with heat-killed *S. pneumoniae* or αCD3 as stimulants. Percentage of $FOXP3^+$ cells are
1240 shown. Data are pooled from separate experiments. * denotes significant differences between
1241 the indicated groups as determined by One-Way ANOVA followed by Šídák's multiple
1242 comparisons test. * is $p \leq 0.05$ and ** is $p \leq 0.01$. Graphs represent the mean +/- SD.

1243

1244

1245

1246

1247

1248

1249

1250

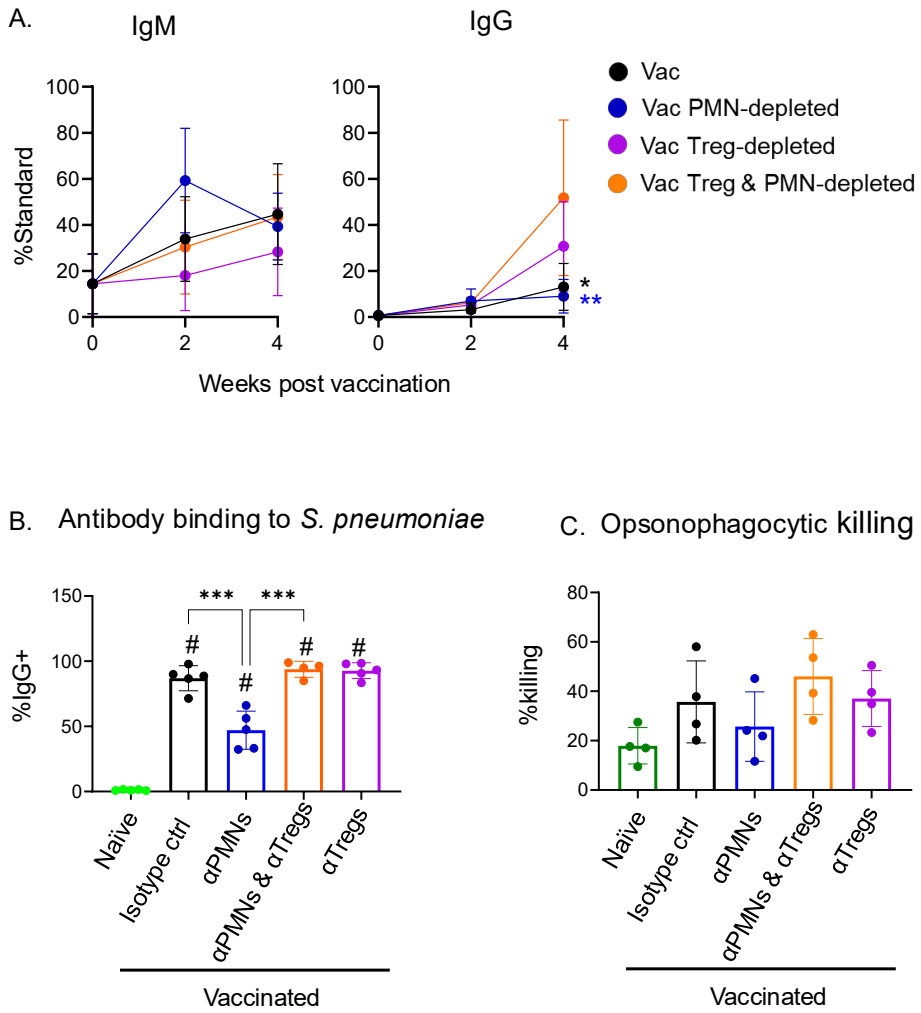

Figure 8: Effect of Treg depletion on antibody responses. Adult C57BL/6 female mice were injected with PCV or PBS and depleted of their PMNs and/or Tregs (αCD25) or treated with an isotype control. (A) Production of IgM and total IgG against type 4 pneumococcal polysaccharides were assessed on weeks 0, 2 and 4 post vaccination. Sera collected 4-weeks post vaccination were used to assess (B) the binding efficacy of antibodies to *S. pneumoniae* using flow cytometry and (C) the ability of antibodies to induce opsonophagocytic killing by PMNs. (A) Data are presented as percentage of standard sera and are pooled from a total of 3 experiments with a total of n=9 mice per group per timepoint. * denotes significant differences between PMNs- & Tregs-depleted mice and group matching the symbol color as determined by Kruskal-Wallis test followed by Dunn's multiple comparisons test. (B) Data are from 5 separate experiments with

each dot representing the average of technical replicates. * denotes significant differences between the indicated groups as determined by One-way ANOVA followed by Šídák's multiple comparisons test and # denotes significant differences from naïve as determined by One-way ANOVA followed by Holm-Šídák's multiple comparisons test. *** is $p \leq 0.001$, and # is $p \leq 0.001$. Bar graphs represent the mean +/- SD. (C) Data are pooled from 3 separate experiments with each dot representing the average of technical replicates from an individual mouse. All line graphs represent the mean +/- 95% confidence interval and all bar graphs represent the mean +/- SD.

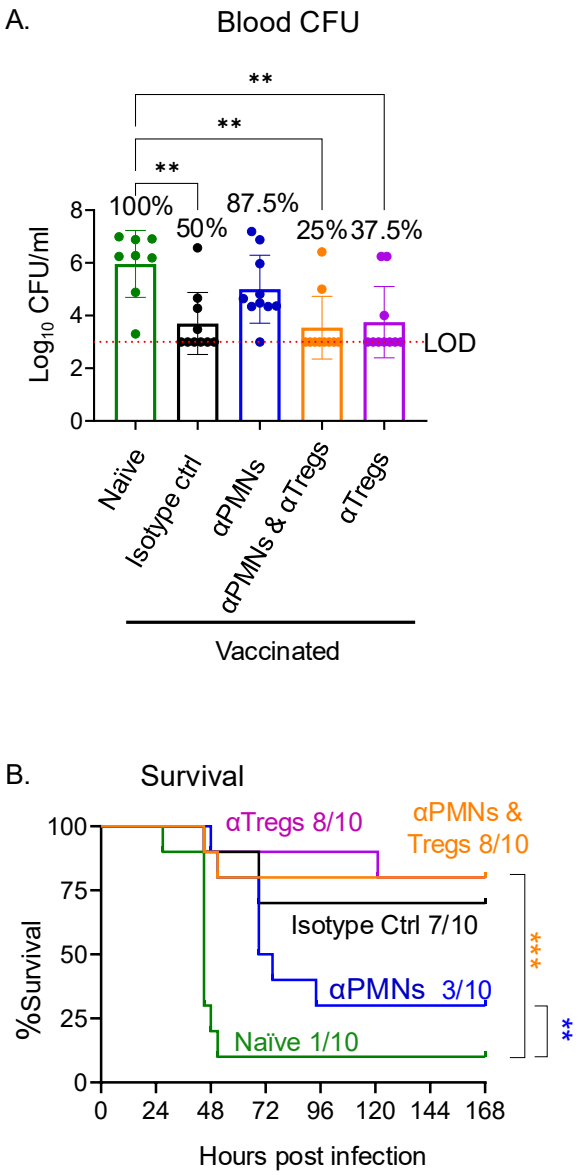

Figure 9: Effect of Treg depletion on the protective efficacy of sera against pneumococcal infection. Adult C57BL/6 female mice were injected with PCV or PBS and depleted of their PMNs and/or Tregs (αCD25) or treated with an isotype control. Sera were collected from all mice 4 weeks post vaccination. Sera from each mouse group was adoptively transferred into a new set of naïve mice which were subsequently infected with $3x10^5$ CFU of *S. pneumoniae*. (A) Bacterial burden in the blood was assessed 45 hours post infection. (B) All mice were monitored for survival for 7 days following infection. (A) Data are pooled from 2 separate experiments and each dot

1294 represents an individual mouse with a total of n=10 mice per group. * denotes significant
1295 differences between the indicated groups as determined by Kruskal-Wallis test followed by Dunn's
1296 multiple comparisons test. Bar graphs represent the mean +/- SD. (B) Data are pooled from 2
1297 separate experiments with a total of n=10 mice per group. * denotes significant differences
1298 between the indicated groups as determined by Mantel-Cox test. ** is $p \leq 0.01$, and ** is $p \leq 0.01$.
1299
1300
1301
1302
1303
1304
1305
1306
1307
1308
1309
1310
1311
1312
1313
1314
1315
1316
1317
1318
1319

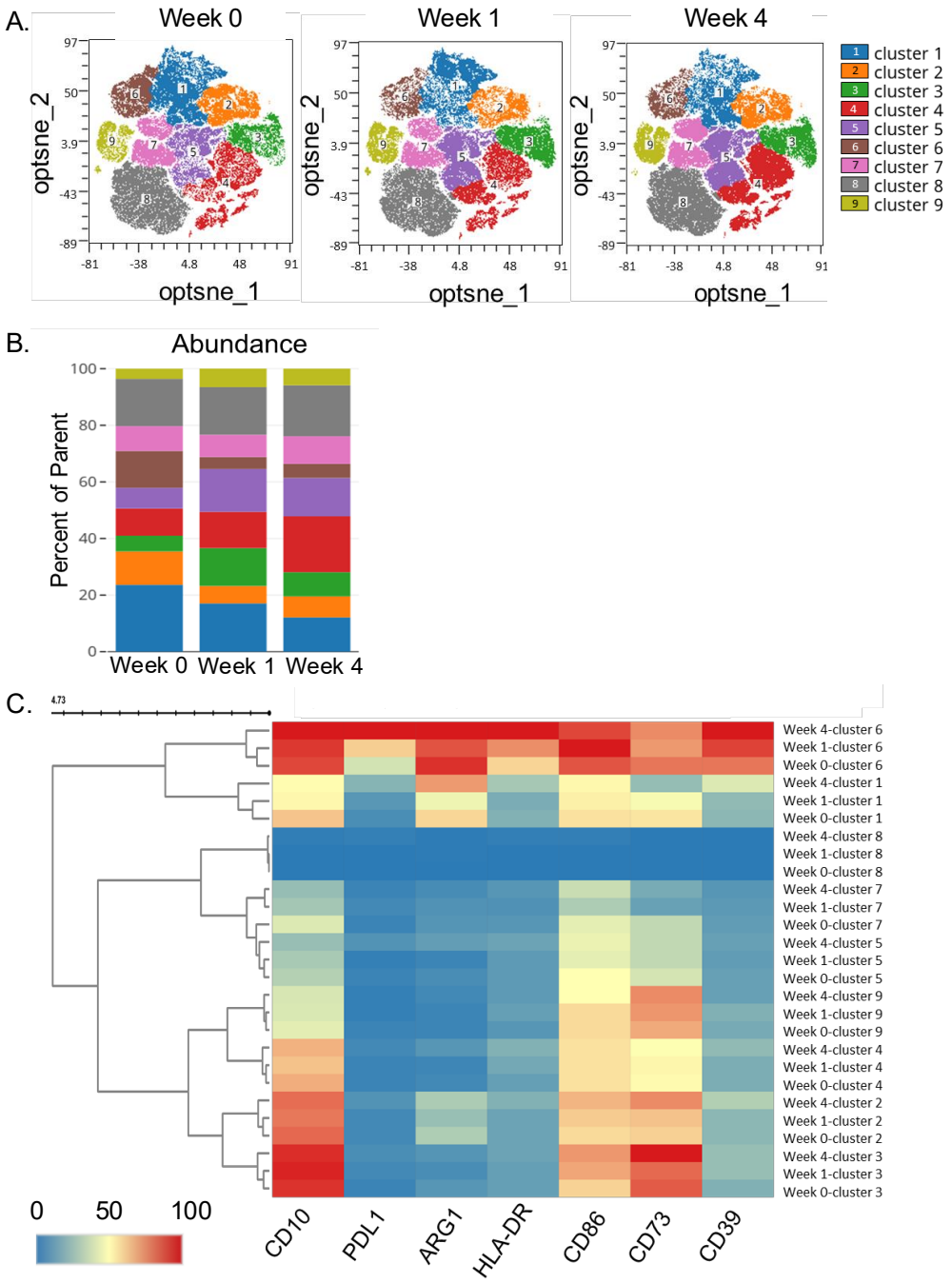

Figure 10: PMN phenotype following PCV vaccination in humans. Young (24-29 years old) female donors were vaccinated with PCV. Blood was collected prior (week 0) to and on weeks 1 & 4 post vaccination. PMNs were isolated from peripheral blood and assessed using flow cytometry. Expressions of HLA-DR, CD10, CD86, PD-L1, ARG1, CD73 and CD39 on PMNs were determined. (A) Clustering of investigated markers throughout the weeks, (B) cluster abundance

1326 throughout the weeks, and (C) heat map of markers throughout the different weeks and clusters
1327 were analyzed using FLOSOM via OMIQ. Data are pooled from six donors.
1328
1329
1330
1331
1332
1333
1334
1335
1336
1337
1338
1339
1340
1341
1342
1343
1344
1345
1346
1347
1348
1349
1350
1351

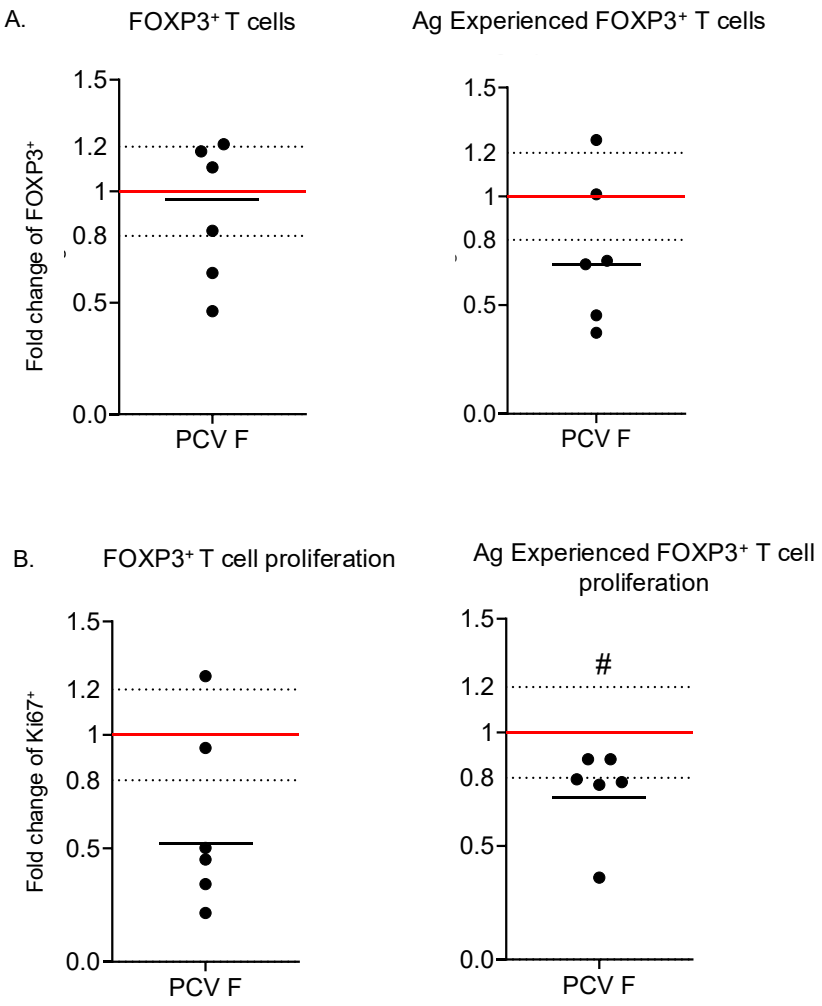

Figure 11: Human PMN and PBMC co-cultures following PCV vaccination. Young (24-29 years old) female donors were vaccinated with PCV. One week post vaccination, PBMCs and PMNs were isolated from peripheral blood. PBMCs were cultured in the presence or absence of matched donor PMNs for 2 days with PCV as a stimulant. (A) Percentage and (B) proliferation of total (left) and antigen experienced (right) FOXP3$^+$ T cells (CD4$^+$) are shown. Data are pooled from six donors and each dot represents a donor. Data are presented as fold change of PBMC divided by PBMC +PMNs conditions. The dashed lines represent a 20% difference in responses between the conditions. Graphs represent the mean, and # indicate significant differences from 1 as measured by a one-sample t-test.